2020

CHARACTERIZING THE ROLES OF PIPECOLIC ACID AND REACTIVE OXYGEN SPECIES METABOLIC ENZYMES IN PLANT SYSTEMIC IMMUNITY

Ruiying Liu
University of Kentucky, ruiying.liu@uky.edu
Author ORCID Identifier:
 https://orcid.org/0000-0002-3133-9205
Digital Object Identifier: https://doi.org/10.13023/etd.2020.212

Right click to open a feedback form in a new tab to let us know how this document benefits you.

CHARACTERIZING THE ROLES OF
PIPECOLIC ACID AND REACTIVE OXYGEN SPECIES METABOLIC ENZYMES
IN PLANT SYSTEMIC IMMUNITY

_____

DISSERTATION

_____

A dissertation submitted in partial fulfillment of the
requirements for the degree of Doctor of Philosophy in the
College of Agriculture, Food and Environment
at the University of Kentucky

By
Ruiying Liu
Lexington, Kentucky
Director: Dr. Aardra Kachroo, Professor of Plant Pathology
Lexington, Kentucky
2020

ABSTRACT OF DISSERTATION

CHARACTERIZING THE ROLES OF
PIPECOLIC ACID AND REACTIVE OXYGEN SPECIES METABOLIC ENZYMES
IN PLANT SYSTEMIC IMMUNITY

Systemic acquired resistance (SAR), initiated by a plant upon recognition of microbial effectors, involves the generation of mobile signals at the primary infection site, which translocate to and activate defense responses in distal tissues. Among the signals contributing to SAR include salicylic acid (SA), nitric oxide (NO), reactive oxygen species (ROS), glycerol-3-phosphate (G3P), and pipecolic acid (Pip). Our previous studies show there are two branches of SAR signaling pathways in Arabidopsis: one regulated by NO/ROS-G3P and the other by SA. Both NO/ROS-G3P and SA-mediated signaling branches function in parallel during SAR. To better understand the role of Pip in SAR and the molecular mechanisms underlying Pip-mediated signaling, I investigated relationship between Pip and other SAR signals. My results suggest that Pip-mediated SAR is dependent on the NO/ROS-G3P branch of the SAR pathway. This is supported by the results that exogenous Pip increases NO, ROS, and G3P, but not SA. Detailed characterization of Pip metabolism showed that Pip acts upstream of several known and unknown derivatives. I also investigated involvement of ascorbic acid biosynthetic enzymes and several ROS scavenging enzymes in SAR. Together, my results suggest that Pip- and ROS-metabolic pathways regulate key steps of SAR signaling in plants.

KEYWORDS: SAR, Pipecolic acid, ROS, SOX, Ascorbic acid, APX

Ruiying Liu
(Name of Student)

05/15/2020
Date

CHARACTERIZING THE ROLES OF
PIPECOLIC ACID AND REACTIVE OXYGEN SPECIES METABOLIC
ENZYMES IN PLANT SYSTEMIC IMMUNITY

By
Ruiying Liu

Dr. Aardra Kachroo
Director of Dissertation

Dr. Rick Bennett
Director of Graduate Studies

05/15/2020
Date

DEDICATED TO MY BELOVED PARENTS

.

ACKNOWLEDGMENTS

TABLE OF CONTENTS

LIST OF TABLES

LIST OF FIGURES

CHAPTER 1

INTRODUCTION

Crops, the natural sources of our food, fiber, biofuels and other products, are essential for our daily life. However, the exploding global population and increasing need for renewable bioenergy raise a worldwide focus about yields of food and energy crops. Moreover, during their life cycle, crop plants are constantly challenged by abiotic stress, such as global climate change and biotic stress like plant infectious diseases. Diseases caused by biotic agents such as fungi, oomycetes, bacteria and viruses cause significant economic losses. Each year, about 15% of production losses (Oerke, 2006, McDonald, 2016) is due to plant infectious diseases which causes the public concerns on controlling plant infectious diseases. A susceptible plant host, a virulent pathogen and a favorable environment are required for disease development. Thereby, the improvement of plant defense against microbial pathogens is needed to facilitate crop improvement. For that, we need to deeply understand the mechanism of plant immune systems, which are how plant hosts sense their pathogen intruders, what antimicrobial defense signals are generated and how the signals are amplified to induce efficient defense.

1.1 Plant immune systems

1.1.1 Pathogen-associated molecular patterns (PAMPs)-triggered immunity (PTI) and effector-triggered immunity (ETI)

In plants, the immune systems are categorized into two types: the innate immunity and systemic immunity. The innate immunity, or called local resistance, can protect plants at infected (local) tissue, whereas the systemic immunity, an acquired immunity induced by a previous infection, can provide the plant with systemic resistance in non-infected (distal) tissue (Shine *et al.*, 2018).

Local resistance includes non-host resistance, basal resistance to virulent pathogens or Resistance protein-mediated resistance to avirulent pathogen isolates (Shine *et al.*, 2018). In general, plants are resistant to most microbes, and only a few microorganisms are considered as plant pathogens because they are capable to cause disease (Lipka *et al.*, 2008). This type of resistance is called nonhost resistance which is not pathogen-race-specific. Non-host resistance is durable but complicated and its utilization in crop improvement need to further study (Gill *et al.*, 2015).

Basal resistance is also termed microbial- or pathogen-associated molecular patterns (MAMPs or PAMPs) triggered immunity (PTI). Once a plant pathogen entering into plant tissue through wounds or natural openings such as stomata, a transmembrane protein named pattern recognition receptor (PRR) in the host plants can recognize MAMPs or PAMPs which consequently triggers PTI (Schwessinger & Ronald, 2012). PAMPs, are small molecular motifs and are conserved within microbial species. The well-known PAMPs include flagellin, lipopolysaccharide and peptidoglycans. Upon recognition of PAMPs, a signaling cascade is activated in the stomatal guard cell to ultimately close

stomata as part of PTI in plants (Melotto *et al*, 2006; Melotto *et al*, 2017). PTI also induces the formation of immune signaling complexes and cascades of defense responses, including activation of mitogen-activated protein kinases (MAPK), production of reactive oxygen species (ROS), induction of immune-related genes, modification of cell wall and others (Zipfel, 2014).

A multi-layer attack and defense relationship between pathogens and their plant hosts is described as a Zig-zag model (Jones and Dangl, 2006). PTI, which is the first layer in this defense system, can be suppressed by pathogen encoded effector proteins (Cui *et al*., 2013; Dangl *et al*., 2013). Pathogens elicit effector proteins into the host cell through type III protein secretion system (T3SS) (Buell *et al*., 2003; Jin *et al*., 2003) to interfere with immune signaling and disrupt defense responses. This phenomenon is called effector-triggered susceptibility (ETS) (Jones and Dangl, 2006).

However, plants have evolved with Resistance (R) proteins to detect specific effectors and activate a second layer of response. This type of immune response is termed R protein mediated resistance or effector-triggered immunity (ETI). The specific effector recognized by R protein is referred to as avirulent (Avr) protein and the pathogen contained Avr protein is referred to as avirulent pathogen. This specific R-Avr protein recognition is well-known as gene-for-gene interaction (Flor, 1971). Most of known plant R proteins contain conserved structural domains, which include N-terminal coiled-coil (CC) or Toll-interleukin 1 receptor (TIR)-like domains, a nucleotide-binding (NB) domain and C-terminal leucine-rich repeat (LRR) domains (Kachroo *et al*., 2006; Martin *et al*., 2009). R protein can recognize Avr via direct interactions between these two proteins or via indirectly regulation through other host proteins (Kachroo *et al*., 2006).

Induction of ETI is often accompanied with a programmed cell death, termed hypersensitive response (HR) at the infection site and also rapid immune signaling transduction with increased levels of endogenous defense-related molecules, such as salicylic acid (SA) and transcriptional upregulation of defense genes (Dangl *et al*., 1996; Durrant & Dong, 2004). Among these defense genes, *Enhanced Disease Susceptibility 1* (*EDS1*) and *Phytoalexin Deficient 4* (*PAD4*) are two critical genes in ETI and their functions are widely studied. Both EDS1 and PAD4 are required for R-mediated resistance to *Turnip crinkle virus* (TCV) in *Arabidopsis thaliana* (Arabidopsis) (Zhu *et al*., 2011). PAD4 is also required for SA mediated *R* gene, *HRT* (*HR to TCV*) induction (Chandra-Shekara *et al*., 2004) and EDS1 interacts with HRT intensifying HRT-mediated HR to TCV (Zhu *et al*., 2011).

To survive, pathogens avoid ETI either by removing the recognized effector gene, or by acquiring additional effectors that suppress ETI. But conversely, natural selection results in a new R gene to recognize the new acquired effecter so that ETI can be triggered again.

1.1.2 Systemic acquired resistance

Besides inducing local defense, ETI also causes a long-lasting and broad-spectrum immune response to a secondary infection in the distal tissues (Shine *et al*., 2018). This type of immune response, which is unique in plants, is referred to as systemic immunity or systemic acquired resistance (SAR) (Ryals *et al*., 1994).

The phenomenon of SAR has been observed for over 100 years. But in 1933, SAR was first described by Chester and termed physiological acquired immunity. Almost 30 years later, in 1961, A. Frank Ross (1961) first published his study that pre-infected tobacco restricted TMV infection and named this inducible systemic resistance as "systemic acquired resistance". Promisingly, the first endogenous signal molecule of SAR, SA, was identified and Pathogenesis-Related (PR) proteins were found to be related to the onset of SAR (Van Loon & Antoniw, 1982). Besides SA, other biological and chemical changes during SAR had been addressed which included cell death, oxidative burst (Low & Merida, 1996), callose and lignin deposition (Vance *et al*., 1980; Kauss, 1987) and phytoalexin accumulation (Dixon, 1986). The SAR marker genes *PR-1*, *PR-2* and *PR-5* were cloned and characterized in Arabidopsis in the early 1990s (Ward *et al*., 1991; Uknes *et al*., 1992).

In the first 20 years of 21st century, due to the breakthrough in new molecular biological, biochemical and microscopical technology, numerous proteins and chemicals were found to be associated with SAR. SAR has been demonstrated to be associated with transport of mobile signal(s) generated at primary infection site (local tissues) to the noninfected part (distal tissues) which requires elaborate and fine balanced choreography among various phytohormones, metabolites, and proteins (Pieterse *et al*., 2009; Pieterse *et al*., 2012; Shine *et al*., 2018).

A number of chemical inducers of SAR have been identified and some of them have been shown to translocate systemically. SAR associated chemicals include, salicylic acid (SA) (Durrant *et al*., 2004; Park *et al*., 2007), free radicals which are nitric oxide (NO) and reactive oxygen species (ROS) (Wang *et al*., 2014; Wendehenne *et al*., 2014), azelaic

acid (AzA) (Jung *et al*., 2009; Yu *et al*., 2013), glycerol-3-phosphate (G3P) (Chanda *et al*., 2011; Mandal *et al*., 2011; Yu *et al*., 2013), Pipecolic acid (Pip) (Návarová *et al*., 2012; Wang *et al*., 2018) and Pip derivative N-hydroxy-pipecolic acid (NHP) (Hartmann *et al*., 2018; Chen *et al*., 2018). Recent results have shown that SA regulates one branch of SAR, whereas AzA, G3P, NO, and ROS regulate the other branch of SAR and both pathways are essential for induction of SAR (Chanda *et al*., 2011; Yu *et al*., 2013; Wang *et al*., 2014; Gao *et al*. 2014; Lim *et al*., 2016). The role of Pip as well as NHP in SAR and its interaction with other SAR chemical inducers will be described in the Chapters 3 and 4.

1.2 Endogenous chemical inducers of SAR

1.2.1 Salicylic acid

SA, 2-hydroxy benzoic acid, is an important phytohormone which has been shown to regulate various aspects of plant growth and development; and it also contributes to both local and systemic resistance and accumulates upon pathogen infection (Vlot *et al*., 2009; Dempsey *et al*., 2011; Kachroo & Kachroo, 2007). Plant mutants defective in biosynthesis, perception or signal transduction of SA often show enhanced disease susceptibility at the infection site and exhibit impaired SAR response. In contrast, plant mutants constantly accumulating high levels of SA exhibit high resistance (Clarke *et al*., 2001; Vlot *et al*., 2009). SA is synthesized via the shikimic acid pathway and derived from chorismic acid. Chorismic acid can be converted to SA via two distinct enzymatic pathways. Both pathways are named based on their key enzymes which are phenylalanine ammonia lyase

(PAL) and isochorismate synthase 1 (ICS1), the product of the *SA-Induction Deficient 2 (SID2)* gene. In Arabidopsis, approximately 98% of pathogen-induced SA is derived from ICS pathway (Wildermuth *et al*., 2001; Shine *et al*. 2016; Torrens-Spence *et al*., 2019). However, unlike in Arabidopsis, in which the ICS pathway is predominant in pathogen-induced SA biosynthesis, in soybean the PAL and ICS pathways function equally for pathogen-induced SA biosynthesis (Shine *et al*. 2016). The ICS pathway has been elucidated recently. The conversion from chorismic acid to isochorismate via ICS1 occurs in the chloroplast (Wildermuth *et al*., 2001) followed by its exportation into the cytosol via the *Enhanced Disease Susceptibility 5* (*EDS5*) gene product, a multidrug and toxin extrusion (MATE) family protein located in the chloroplast envelope (Rekhter *et al*., 2019a; Torrens-Spence *et al*., 2019; Serrano et al., 2013). Once isochorismate is transported into the cytosol, it conjugates with glutamate to form isochorismate-9-glutamate by the function of a cytosolic aminotransferase, which is the product of *avrPphB Susceptible 3* (*PBS3*) gene, and then the conjugate spontaneously decomposes into SA and 2-hydroxy-acryloyl-N-glutamate (Rekhter *et al*., 2019a; Torrens-Spence *et al*., 2019). Except free SA in cytosol, most of SA is conjugated with glucose as an inactive form, salicylic acid 2-O-β-glucoside (SAG) (Dempsey *et al*., 2011). SA accumulation and signaling also involves additional components including EDS1 (Zhu *et al*., 2011), PAD4 (Jirage *et al*., 1999; Zhu *et al*., 2011), and NPR1/3/4 (the products of *Non-expressor of Pathogenesis-Related gene 1/3/4 genes*) (Cao *et al*., 1997; Ding *et al*., 2018). Exogenous application of SA or its biologically active analogues is sufficient to induce the expression of many defense genes such as *PR1* and confers enhanced local resistance and SAR (Vlot *et al*., 2009). Recent analysis has suggested that local- to distal-translocation of SA likely

occurs via the apoplast (Lim *et al*., 2016). This is based on the results that pathogen infection leads to higher SA levels in the apoplastic compartment while translocation of SA is not affected by impaired symplastic transport via plasmodesmata (PD) (Lim *et al*., 2016).

1.2.2 Free radicals

NO is a gaseous molecule and highly diffusible in the cell and has emerged as a key signaling molecule in bacteria, plants and animals. NO regulates many physiological processes in plants directly or by S-nitrosylation (post translational modification of cysteine residues to S-nitroso-cysteine) of key proteins (Shine *et al*., 2018). In plant defense, the translocation of NPR1 from cytosol to nucleus is associated with the S-nitrosylation of NPR1 (Lindermayr *et al*., 2010). And S-nitrosylation of NPR1 facilitates its oligomerization, which maintains protein homeostasis upon SA induction (Tada *et al*., 2008). Our previous data showed NO is associated with SAR and NO-induced SAR is highly concentration dependent (Wang *et al*., 2014). Too low or too high levels of NO can inhibit SAR. A major source of NO production in plants is from nitrate via nitrate reductases (Chamizo-Ampudia *et al*., 2017). In Arabidopsis, there are two nitrate reductases, nitrate reductase 1 (NIA1) and nitrate reductase 2 (NIA2*)* (Wilkinson *et al*., 1993), which are functionally non-redundant in SAR (Wang *et al*., 2014). Besides, a GTPase, the product of *NO Associated Protein 1 (NOA1)* gene, also contributes to generate NO via an unknown mechanism and is partially functionally redundant with the NIA isoforms (Crawford 2006; Mandal *et al*., 2012; Gaupels *et al*., 2017). Thus, *noa1 nia1* or

noa1 nia2 double mutant plants are fully compromised in pathogen-induced NO accumulation and the onset of SAR (Wang *et al*., 2014; Mandal *et al*., 2012). Another free radical, reactive oxygen species (ROS), including peroxide, superoxide, hydroxyl radical, singlet oxygen and hydrogen peroxide (H_2O_2), are also required for SAR. Like NO, ROS-mediated SAR is also concentration-dependent (Wang *et al*., 2014). ROS can be generated in many ways and it is a common byproduct during oxidation reactions. One way that contributes to ROS biosynthesis is via respiratory burst oxidase homologs (RBOH). Two of RBOH proteins, RBOHD and RBOHF are associated with SAR-related ROS generation and thereby mutant *rbohD* and *rbohF* are defective in SAR (Wang *et al*., 2014). Pathogen-induced NO accumulation is also reduced in *rbohD* and *rbohF* plants (Wang *et al*., 2014). NO application is unable to confer SAR in the *rbohD* and *rbohF* mutants, but ROS is able to confer SAR in *noa1 nia2* mutant plants, suggesting that ROS acts downstream of NO. However, the *rbohD* and *rbohF* mutants accumulate reduced amounts of NO, suggesting that ROS and NO operated in a feedback loop in plants (Wang *et al*., 2014).

1.2.3 Azelaic acid

Azelaic acid (AzA) is a C9 dicarboxylic acid derived from the hydrolysis of C18 fatty acids (FAs) like oleic acid (18:1) and/or its desaturated derivatives, linoleic acid (18:2) and linolenic acid (18:3) present on the galactolipids monogalactosyldiacylglycerol (MGDG) and digalactosyldiacylglycerol (DGDG) (Yu *et al*., 2013). The C18 FAs 18:1, 18:2, and 18:3 contain a double bond on C9, which is eventually converted to AzA after

cleavage (Yu *et al*., 2013). ROS functions to oxidize the double bond on C9 of C18 unsaturated FAs, resulting in the generation of AzA.

Besides serving as a precursor for AzA, the DGDG also functions at an upstream step in SAR where it is required for pathogen-induced NO and SA biosynthesis (Gao *et al*., 2014). The biosynthesis of MGDG and DGDG lipids is catalyzed by the plastidal enzymes MGD1 and DGD1, respectively. The mutant *dgd1* is defective in AzA, NO and SA accumulation and compromised in SAR, however, petiole exudates from pathogen-infected *dgd1* plants were able to confer SAR in wild-type plants, suggesting that SAR signal(s) upstream of SA and NO branches are present in the *dgd1* plant and can induce SA and NO levels in plants containing normal level of DGDG lipid. Moreover, replacing the terminal galactose sugar in DGDG with glucose restored the morphological and photosynthesis defects in *dgd1* plants but still was unable to restore pathogen induced NO or SA accumulation and SAR (Gao *et al*., 2014) which emphasizes the importance of the terminal galactose sugar moiety in SAR signaling.

1.2.4 Glycerol-3-phosphate

G3P is synthesized via phosphorylation of glycerol catalyzed by glycerol kinase (encoded by *Glycerol-Insensitive 1*, *GLI1* gene) or reduction of dihydroxyacetone phosphate mediated by G3P dehydrogenase (encoded by *GLY1* gene). Mutant lost the function of *GLI1* or *GLY1* is defective in G3P biosynthesis and loss the ability of SAR (Chanda *et al*., 2011; Chanda *et al*., 2008). G3P-mediated signaling is dependent on a lipid transfer protein (LTP), DIR1 (the product of *Defective in Induced Resistance* gene), and

an LTP-like protein, AZI1 (the product of *AzA-Insensitive* gene) (Jung *et al*., 2009; Yu *et al*., 2013). DIR1 and AZI1 interact with each other, and G3P is required for DIR1/AZI1 transcript stability (Yu *et al*., 2013, Chanda *et al*., 2008). Conversely, DIR1 and AZI1 are required for avirulent pathogen inducible G3P accumulation, suggesting that G3P and DIR1/AZI1 regulate SAR via a feedback loop (Gao *et al*., 2014).

AzA induces the biosynthesis of G3P, and consequently, exogenous AzA is unable to confer SAR on *gli1* and *gly1* mutants (Yu *et al*., 2013). And also, AzA requires DIR1 and AZI1 for SAR induction (Jung *et al*., 2009), suggesting that AzA is on the upstream of G3P-DIR1/AZI1 feedback loop. Unlike SA, both AzA and G3P, are transported though PD and their translocation from local to distal tissues is significantly reduced in plants that show reduced PD permeability (Lim *et al*., 2016).

1.3 Key findings

In my dissertation, I show that Pip confers SAR via regulating the generation of free radicals, ROS and NO, and functions upstream of NO-ROS-AzA-G3P branch of SAR pathway. However, both SA and G3P are required for Pip accumulation in the distal tissues. Flavin-containing monooxygenase 1 (FMO1) and sarcosine oxidase (SOX) are two enzymes in Pip metabolism. My studies show that FMO1 mutation or SOX overexpression in Arabidopsis result in compromised SAR, which implies that Pip catabolism is involved in SAR signaling. My studies also show that exogenously applying Pip in Arabidopsis enhances plant resistance but does not increase *PR* gene level, indicating that application of Pip on to the crops will not have a negative impact on yield.

So, Pip is an ideal immunity inducer to be utilized onto crops. To deep understand the mechanism of Pip mediated SAR will help us use Pip with effect to protect plants from diseases.

The other part of my research is to understand the mechanism of ROS in regulating SAR, I characterized the role of ascorbic acid biosynthetic enzymes and several ROS scavenging enzymes, ascorbate peroxidase (APX) in SAR. The data show that mutant defect in ascorbic acid biosynthesis results in accumulation of Pip level and in addition, Pip confers SAR on several SAR-deficient APX mutants. Together, these data enhance the connection between Pip and ROS in SAR and highlight their coordination in the induction of SAR.

CHAPTER 2

MATERIAL AND METHODS

2.1 Plant growth conditions

Arabidopsis seeds were sown on bedding plant containers (Hummert International, USA) filled with soil and subjected to cold treatment at 4 °C overnight for synchronized germination. The next day, seeds were transferred into a MTPS 144 (Conviron, Canada) walk-in chamber. Two weeks after germination, the Arabidopsis seedlings were transplanted into individual pots (4 seedlings per pot). The soil used in this study was premixed with commercial soil mixture (PROMIX, Premier Horticulture Inc., Canada) and fertilizer (JR Peters, USA) before use. The plants were grown at 22 °C, 65% relative humidity and 14 h photoperiod. The photon flux density (PFD) of the light period was ~106.9 μmoles·m^{-2}·s^{-1} (measured by digital light meter, Phytotronics Inc., USA).

2.2 Mutant screening and genetic analysis

The seeds for mutants used in this study were obtained from Arabidopsis biological resource center (ABRC, USA) or GABI-Kat (Germany). The genotype information is listed in Table 2.1. To conform the genotype, plant genomic DNA was used as template in PCR. Homozygous T-DNA insertion lines were identified by PCR products with the specific primer for the T-DNA left border in combination with-gene-specific primers.

EMS mutant *vtc1* and *sid2*, was identified by derived(d)-CAPS or CAPS analysis. The primers used for genotyping are list in Table 2.2.

Crosses were performed by emasculating the flowers of the recipient genotype and pollinating with the pollen from the donor. Homogenous F2 generation were selected by genotyping while wild-type and parent mutant alleles were used as control.

2.3 DNA extraction

About 5 mm×5 mm square of leaf tissue was taken in a small-scale DNA extraction. Leaf samples were frozen in liquid nitrogen and grounded with nucleotide-free plastic pestle (Fisher Scientific, USA). The grounded tissue was suspended in 150 μL of DNA extraction buffer (200 mM Tris pH8.0, 25 mM EDTA, 1% SDS and 250 mM NaCl). The homogenate was mixed with 75 μL of phenol: chloroform: isoamyl alcohol (25: 24: 1) mixture and centrifuged for 10 min at 12,000 rpm. 120 μL of the supernatant was transferred into a new tube and precipitated with 80 μL of isopropanol. After centrifuging at 12,000 rpm for 10 min, liquid was discarded, and the DNA pellet was left in the tube. The DNA was air-dried and resuspended in 100 μL of sterile milli-Q water.

2.4 RNA extraction

About 100 mg of leaf tissues were sampled and frozen in liquid nitrogen immediately. Samples was grounded with nucleotide-free plastic pestle and suspended in 1 mL of TRIzol reagent (Invitrogen, USA). The homogenate was mixed with 200 μL of

chloroform, then vortexed for 10 s and centrifuged at 12,000 rpm for 10 min. Supernatant

was transferred into a new tube and precipitated with 500 µL of isopropanol. Placing the

mixture at -20 °C for 1 h, then the mixture was centrifuged at 12,000 rpm for 10 min. The

liquid was discarded. RNA precipitate was washed with 75% alcohol, air-dried and

resuspended in 20 µL of DEPC- treated milli-Q water.

RNA concentration was determined either via UV spectrophotometer (Thermo

electron corporation, USA) or NanoDrop spectrophotometer (Thermo Scientific, USA).

To determine RNA concentration via UV spectrophotometer, an Absorption 260 (A260)

reading of 1.0 was equivalent to ~40 µg/mL single-stranded RNA and the A260/A280

ratio was used to assess RNA purity. 7 µg of total RNA was performed for gel

electrophorese. Before loading, RNA was mixed with 20 µL denature mixture (1mg/mL

ethidium bromide, 0.39×MOPS, 13.7% formaldehyde and 39% formamide), heated at 65

°C for 15 min and chilled on ice for 5 min. The gel was prepared with 1.5% agarose gel

containing 3% formaldehyde and 1×MOPS.

2.5 Reverse transcriptase-polymerase chain reaction (RT-PCR) and real-time quantitative RT-PCR (qPCR)

Total RNA was extracted as described above and 5 µg total RNA was carried out

to synthesize the first strand cDNA. To anneal to primer, RNA was first mixed with 1 µL

oligo dT-17 primer (0.5 µg/µL) and DEPC water to make the total volume reaching to 11

µL and then placed in 65 °C water bath for 15 min. After chilling on ice for 5 min, 2 µL

100 mM DTT, 1 µL 10 mM dNTPs, 1 µL RNAse inhibitor (40 U/ µL, Invitrogen, USA),

1 µL reverse transcriptase (200 U/µL, Invitrogen, USA) were mixed with previous RNA mixture to set up for the reaction and the reaction was incubated at 42 °C water bath for 1 h. Then the reaction was stopped by heating the mixture in 65 °C water bath for 15 min. The total volume was diluted into 100 µL by adding 80 µL of DEPC water. The RT-PCR was processed for 26 cycles with *β-TUBULIN* primers or *ACTIN* primers to determine absolute levels of transcripts.

The qPCR was carried out as Chanda *et al*. (2011). Each cDNA sample was run in triplicates and *ACTIN* expression levels were used as internal control for normalization. Cycle threshold values were calculated by SDS 2.3 software. Gene-specific primers used for qPCR analyses are described in Table 2.2.

2.6 Gene clone and construction of gene expression vector

pDNOR-*SOX* construct was obtained from my colleague of our lab. After confirmation the SOX fragment sequence by PCR and sequencing, the *SOX* fragment was recombined into upstream of *GFP* gene in pGWB5 binary vector (Nakagawa *et al.,* 2007). pGWB5-*SOX* was transformed into *Agrobacterium tumefaciens* (*A. tumefaciens*) stain MP90. pET28a-*SOX* was obtained from my colleague of our lab and it was transformed into *Escherichia coli* (*E. coli*) strain Rosetta (DE3).

2.7 Bacterial transformation

Heat shock method was used for *E. coli* strain (Omni max, Top 10 or Rosetta) transformation. To prepare heat-shock competent cells, a single isolated colony of *E. coli* was growing overnight in 5 mL Luria-Bertani (LB) broth at 37 °C shaker with the speed of 200 rpm. The overnight-grown culture was regrown in a new fresh LB broth to OD of 0.5 (A600) (the ratio for inoculum: broth is 1: 100) and chilled on ice for 30 min. The cells were collected at 3,000 rpm for 10 min at 4 °C and resuspended in ice-cold Tfb I buffer (30 mM KAc pH 5.8, 100 mM $RbCl_2$, 10 mM $CaCl_2$ and 15% glycerol, the ratio for inoculum: Tfb I buffer is 1: 50). The cells were chilled on ice for 30 min and then centrifuged at 3,000 rpm for 10 min. The collected pellet was suspended in ice-cold Tfb II buffer (10 mM MOPS pH 6.5, 75 mM $CaCl_2$, 10 mM $RbCl_2$, 15% glycerol, the ratio for inoculum: Tfb II buffer is 1: 5). After 15 min on ice, the cells were dispensed as 100 µL aliquots in 1.5 mL microfuge tubes, frozen in liquid nitrogen immediately and stored at -80 °C for future use. For heat-shock transformation, plasmid DNA was mixed with 100 µL of competent cells, incubated on ice for 15 min, followed by heat shock at 42 °C for 90 sec. The transformed cells were chilled on ice for 5 min and then mixed with 600 mL LB broth with no antibiotic and incubated at 37 °C for 45 min. The transformed cells were centrifuged at 5,000 rpm for 30 sec and then plated on LB agar plates containing appropriated antibiotic. The plates were incubated at 37 °C overnight. Positive colonies were identified by colony PCR and regrown in LB broth for the plasmid extraction. Plasmid extraction was carried out by using QIAprep Spin Miniprep Kit (QIAGEN, USA). Plasmids were sent to Eurofins Genomics LLC for sequencing.

Electroporation method was used for *A. tumefaciens* (MP90) transformation. To prepare electroporation competent cells, a single isolated colony of *A. tumefaciens* strain

was cultured overnight in 5 mL LB broth at 29 °C shaker with the speed of 250 rpm. The overnight-grown culture was regrown in a new fresh LB broth to OD of 0.5 (A600) (the ratio for inoculum: broth is 1: 100) and chilled on ice for 30 min. The cells were collected at 3,000 rpm for 10 min at 4 °C and resuspended in ice-cold 8.0% glycerol (the ratio for inoculum: 8.0% glycerol is 1: 50). The cells were dispensed as 20 µL aliquot in 1.5 mL microfuge tubes, frozen in liquid nitrogen immediately and stored at -80 °C for further use. For electroporation transformation, plasmid DNA was mixed with 20 µL of competent cells and placed in a cuvette and given a pulse at 2,500 volts (12.5 kV/cm). The mixture was inoculated into 1 ml LB broth and incubated for 1 h at 29 °C. The treated cells were plated on LB agar plates containing appropriate antibiotic and incubated for two days at 29 °C. The positive transformants were identified by colony PCR.

2.8 Generation of transgenic plants

Col-0 or mutant plants using floral dip method (Clough & Bent, 1998). *A. tumefaciens* stain MP90 containing pGWB5-*SOX* was used for transformation. The transgenic plant seeds were selected on ½ Murashige and Skoog (MS) medium plate containing 17 µg/mL hygromycin. The transgenic plant was confirmed by genotyping analysis and confocal microscope analysis of the T1 plants and analyzing the GFP level in the T2 generation.

2.9 Protein extraction

50-200 mg fresh plant tissues were frozen by liquid nitrogen immediately, grounded with plastic pestle, and then homogenized with 50 µL protein extraction buffer. For Arabidopsis protein extraction, the extraction buffer contains 10% glycerol, 50 mM Tris-Cl pH 7.5, 1 mM EDTA, 150 mM NaCl, 0.1% Triton-X, and 1% plant protein inhibitor (Sigma). And for *N. Benthamiana* protein extraction, the buffer contains 10% glycerol, 50 mM Tris-Cl pH 7.5, 1 mM EDTA, 150 mM NaCl, 0.1% Triton-X, 2% PVPP (W/V) and 1% plant protein inhibitor (Sigma). The extract was centrifuged at 12,000 rpm for 15 min at 4 °C and the supernatant was transferred into a new tube. This process was repeated one more time. The protein concentration was determined by Bio-Rad protein assay dye via the measurement of spectrophotometer (diverse concentration of BSA solutions and corresponding A595 value was utilized to plot the standard curve and protein concentration was cross-referred from the curve).

2.10 Western blot analysis

25-100 µg total protein was mixed with 10 µL loading buffer (3.0 mL H_2O, 1.2 mL 1 M Tris-HCl pH 6.8, 2.4 mL glycerol, 0.48 g SDS, 60 µL 10% bromophenol blue and 1.5 mL β-mercaptoethanol) and boiled at 100 °C for 5 min before loading into SDS-PAGE gel (the concentration of SDS-PAGE gel was determined by the size of the protein). The samples were run at 90- 150 V in 0.5 or 1×running buffer (14.4 g glycine, 3 g Tris-base and 1 L H_2O). The time for running the gel was determined by the size of the protein.

PVDF membrane (Immun-Blot, Bio-Rad) was pre-wet in methanol and other materials were pre-wet in 1× transferring buffer (3.2 g Tris-base, 15 g glycine and 1 L

H$_2$O). The materials were stacked in the transferring case (following the order: sponge, Whatman paper, membrane, protein gel, Whatman paper, sponge). The protein gel was transferred at 400 mA for 1 h on ice with the Bio-Rad mini-gel electro transfer box. After transferring, PVDF membranes were stained with Ponceau-S solution (40% methanol, 15% acetic acid, and 0.25% Ponceau-S). The membranes were distained by deionized water for 2-4 times.

For western blotting analysis, the membrane was first blocked in 10 mL 1×TBST buffer (5 mM Tris-base, 20 mM NaCl, pH 7.4, and 0.1% TWEEN 20) containing 5% non-fat dry milk for 1 h on a shaker at the room temperature. After blocking, the primary antibody was added into fresh 10 mL 1×TBST buffer with 5% non- fat dry milk and incubated on a shaker for 4 h at the room temperature or overnight at 4 °C. The membrane was washed 4-7 times for 5 min with 1×TBST buffer, and then incubated in 1×TBST buffer with 5% non-fat dry milk and the secondary antibody (HRP-conjugated, Sigma) on a shaker for 2 h. The membrane was washed for 4-7 times for 5 min with 1×TBST buffer, developed with ECL kit (1 mL per membrane) (Super-Signal, Thermo Scientific) and exposed to autoradiography film (Santa Cruz Biotechnology, USA).

2.11 Protein localization

To determine protein localization, the transgenic Arabidopsis leaves as described before were carried out for confocal microscopy analysis. For confocal imaging, about 5 mm×5 mm water-mounted leaf sections were examined by an Olympus FV 1000 confocal microscope (Olympus America, Melvile, NY) using a water immersion

PLAPO60XWLSM2 (NA 1.0) objective. GFP were excited using 488 nm laser lines. Olympus FLUOVIEW 1.5 was used to control the microscope.

2.12 Pathogen infection: *Pseudomonas syringe* pv. *Tomato*

The *Pseudomonas syringe* pv. *Tomato* (*Pst*) strain DC3000 containing pVSP61 (empty vector), or *Pst* avirulent isolate, *avrRpt2* containing pVSP61-*avrRpt2* were grown overnight in King's B broth containing 25 µg/mL rifampicin (Sigma-Aldrich) and 50 µg/mL kanamycin (Sigma-Aldrich). The cells were collected at 5,000 rpm for 2 min, washed and resuspended in 10 mM $MgCl_2$ solution. The bacterial suspension was quantified using spectrophotometer (A600) and diluted to a final concentration of 10^5, 10^6 or 10^7 CFU (colony-forming units)/mL and used for infiltration. The bacterial suspension was injected into the abaxial surface of the leaf using a needle-less syringe.

For SAR assay, mock control plants were injected with 10 mM $MgCl_2$ solution and SAR treated plants were injected with 10^7 CFU/mL *Pst avrRpt2* bacterial. Two days later, three systemic leaves were infiltrated with 10^5 CFU/mL *Pst* DC3000 on both mock and SAR treated plants. Four replicates (three leaf discs per replicate) from each inoculated genotype were collected at 0 and 3 dpi. The leaf discs were homogenized with 1 mL 10 mM $MgCl_2$ solution and 1/10 (for 0 dpi) or $1/10^4$ (for 3 dpi) of homogenate was plated on King's B medium containing 50 µg/mL Rifampicin to grow the *Pst* DC3000. Two days later, the colony number of *Pst* DC3000 was counted and converted into the log value of CFU per cm^2 leave for comparison. In the SAR assay, Arabidopsis plants which were six-week-old age after germination were utilized in the experiments unless noted otherwise.

2.13 Collection of phloem exudate

Leaf exudate was collected as described (Maldonado *et al*., 2002). The plants were induced for SAR by inoculating with *Pst avrRpt2* (10^6 CFU/mL). 8 h-12 h later, leaf petioles were excised, surface-sterilized in 50% ethanol, and 0.05% bleach, rinsed in 1 mM EDTA and submerged in 1.5 mL 1 mM EDTA (containing 100 μg/mL ampicillin). The phloem exudates were collected up to 48 h in a small 20 cm× 20 cm× 20 cm glass chamber. $MgCl_2$ infiltrated leaf petioles were used to collect phloem exudate in the same method to use as control here.

2.14 SA, BTH, NO donor, NO$_2$ donor, ROS, AzA, G3P, Pip, NHP treatments

For SAR assays, SA (500 μM, pH 7.0; Sigma), BTH (100 μM; CIBA-GEIGY Ltd), NO donor (DETA 100 μM; Sigma), NO_2 donor (SULFO 100 μM; Sigma),ROS (H_2O_2 300 μM; Fisher Scientific), G3P (100 μM; Sigma), Pip (1,000 μM; Alfa Aesar, China) and NHP (1,000 μM; Chen *et al.,* 2018) were prepared in sterile water. AzA (100 μM; Sigma) was first dissolved in 200 μL methanol and then diluted into 100 μM with sterile water.

2.15 Extraction and quantification of salicylic acid (SA) and salicylic acid glucoside (SAG)

SA and SAG level were determined by extracting these metabolites from about 0.1 g leaves as described earlier (Chandra-Shekara *et al.,* 2006).

2.16 Extraction and quantification of pipecolic acid (Pip)

Pip level was determined by extracting these metabolites from about 0.1 g leaves as described earlier (Wang *et al.,* 2018).

2.17 Protein purification

A single colony of recombinant *E. coli* BL21 Rosetta cells containing full length *SOX* gene inserted into pET28a vector was picked and cultured overnight in 5 mL LB broth containing 50 µg/mL kanamycin at 37 °C shaker with the speed of 200 rpm. The overnight-grown culture was regrown in a new fresh 500 mL LB broth until the OD_{600} reached to 0.5-0.8. After the culture cooled down, the transgene expression was induced with 0.5 mM isopropyl-β-ᴅ-1-thiogalactopyranoside (IPTG), and the culture was incubated again overnight at 25 °C shaker with the speed of 200 rpm. The bacterial cells were collected by centrifugation at 4,000 rpm for 15 min at 4 °C. The rest steps for protein purification was carried out by using Protino ®Ni-TED columns Kit (Machery-Nagel, Germany).

2.18 ROS staining

For ROS staining, the whole Arabidopsis leaves were stained with 3,3´-diamoinobenzidine as described earlier (Daudi & O'Brien, 2012).

Table 2.1 Seed materials used in this study

No.	Mutants and transgenic seeds	References
1	Columbia-0 (Col-0)	Kachroo *et al.*, 2003
2	*ald1*	Návarová *et al.*, 2012
3	*fmo1*	Návarová *et al.*, 2012
4	*sox*	This study
5	*35S-SOX-GFP*::Col-0	This study
6	*vtc1*	Veljovic-Jovanovic *et al.*, 2001
7	*vtc2*	This study
8	*apx1*	This study
9	*s-apx*	This study
10	*t-apx*	This study
11	*sid2*	Zhu *et al.*, 2013

Table 2.2 List of primers used in the study

No.	Name	Primer sequence	Purpose
1	Salk_007673 (*ald1*) LP	GTTATTTGCTCTGGAATAGGC	Genotyping
2	Salk_007673 (*ald1*) RP	TTTTAAATGGAACGCAAGGAG	Genotyping
3	Salk_026163 (*fmo1*) LP	ATTATTGGGTGTGGGGCTTACC	Genotyping
4	Salk_026163 (*fmo1*) RP	CTGCTTTGGACGTATCCTACG	Genotyping
5	GABI_680F04 (*sox*) LP	CCTTTGGTCCAGCACTACTTG	Genotyping
6	GABI_680F04 (*sox*) RP	TGGGGAAGGGGTAATAGTCTG	Genotyping
7	Salk_017108 LP	CTGCATGAGAATCCATAACC	Genotyping
8	Salk_017108 RP	TTGAAACTCCCATGCAACTTC	Genotyping
9	*vtc1* dCAPS Fwd	TGCATTTTCAGGAAAAGGAGTT	dCAPS (StyI)
10	*vtc1* dCAPS Rev	TTAGCAAAATCAACAAGGGGCCTTG	dCAPS (StyI)
11	CS876707 (*vtc2*) LP	CTTCCGATCTCCTCTTTCTCG	Genotyping
12	CS876707 (*vtc2*) RP	GAGGCAAGCAGTCAAGAACAC	Genotyping
13	Salk_088596 (*apx1*) LP	AAAACGGTTTTAGAGAAGCGC	Genotyping
14	Salk_088596 (*apx1*) RP	AACTCTTGAGCGGAGAGAAGG	Genotyping
15	Salk_000249 LP	CCACCCTGGAAGAGAGGTTAG	Genotyping
16	Salk_000249 RP	CAACGGATGTGTTCAAATCG	Genotyping
17	Salk_083737 (*s-apx*) LP	TTTCGTGATGCAGAATTCAATC	Genotyping
18	Salk_083737 (*s-apx*) RP	CAGAATTTGGTGCTGAGAAGC	Genotyping
19	CS325715 LP	TAACCCGTCACCATTACCATC	Genotyping
20	CS325715 RP	CAGAATTTGGTGCTGAGAAGC	Genotyping
21	Salk_027804 (*t-apx*) LP	ACAAGATCAAACCCACGAATG	Genotyping
22	Salk_027804 (*t-apx*) RP	TACTTCACCAAGATGGGATGG	Genotyping
23	*sid2* CAPS Fwd	CTGTTGCAGTCCGAAAGACGA	CAPS (MfeI)
24	*sid21* CAPS Rev	CTAGAGCTGATCTGATCCCGA	CAPS (MfeI)

Table 2.2 List of primers used in the study (continued)

No.	Name	Primer sequence	Purpose
25	Lbb1.3 (Salk line)	GCGTGGACCGCTTGCTGCAACT	Genotyping
26	Lbb (Sail line)	GCCTTTTCAGAAATGGATAAATAGC CTTGCTTCC	Genotyping
27	Lbb (GABI line)	ATATTGACCATCATACTCATTGC	Genotyping
28	*GFP* Fwd	ATGGTGAGCAAGGGCGAGGAG	Genotyping
29	*GFP* Rev	TCACTTGTACAGCTCGT	Genotyping
30	*β-TUBULIN* Fwd	CGTGGATCACAGCAATACAGAGCC	RT-PCR
31	*β-TUBULIN* Rev	CCTCCTGCACTTCCACTTCGTCTT C	RT-PCR
32	*ACTIN*-qPCR Fwd	CACTGTGCCAATCTACGAGGGTT	qPCR
33	*ACTIN*-qPCR Rev	ACAATTTTCCCGCTCTGCTGTTGTG	qPCR
34	*ALD1*-qPCR Fwd	GGATTGGCATGCCTTTCTTC	qPCR
35	*ALD1*-qPCR Rev	TGAACCCACAAGTATGGAGC	qPCR
36	*PR1*-qPCR Fwd	CACATCCGAGTCTCACTGAC	qPCR
37	*PR1*-qPCR Rev	CAGACTCATACACTCTGGTG	qPCR
38	*SOX attB* Fwd	AAAAAGCAGGCTTATCATTTTCCAC TGCAACAGCT	RT-PCR
39	*SOX attB* Rev	AGAAAGCTGGGTATGCTGAGATTTT TCCTCACCA	RT-PCR

CHAPTER 3

PIPECOLIC ACID CONFERS SYSTEMIC IMMUNITY BY REGULATING

FREE RADICALS[Ψ]

3.1 Introduction

Pipecolic acid (Pip) also called piperidine-2-carboxiylic acid or pipecolate, is a non-protein amino acid and an intermediate in the L-Lysine (Lys) degradation pathway (Návarová *et al*., 2012). In plants, Pip accumulates upon pathogen infection in both local and distal leaves and exogenous application of Pip enhances both PTI and ETI in wild type (WT) Arabidopsis plants (Návarová *et al*., 2012).

The conversion of Lys to Pip in Arabidopsis is catalyzed by an aminotransferase encoded by *AGD2-Like Defense response protein 1* (*ALD1*) gene, which requires pyridoxal-5′-phosphate (PLP) for its activity (Sobolev *et al*., 2013). In the *ALD1* knockout mutant *ald1*, pathogen-induced Pip biosynthesis is shut down in both local and distal leaves (Návarová *et al*., 2012). ALD1 transfers the α-NH$_2$-group of L-Lys to an acceptor, possibly its cofactor PLP (Sobolev *et al*., 2013) or other oxoacids such as pyruvate (Hartmann *et al*., 2017). ALD1 catalyzes the conversion of lysine into Δ^1-piperideine-2-carboxylic acid (P2C). P2C is then converted to Pip via a ketimine reductase encoded by *SAR-Deficient 4* (*SARD4,* alias *ORNCD1*) gene, the closest homolog to the human ketimine reductase CRYM, as verified by both biochemical characterization of *in vitro* SARD4 enzymatic assay and metabolic analyses of *sard4* knockout plants (Ding *et al*., 2016; Hartmann *et al*., 2017). ALD1 is localized in chloroplast (Cecchini *et al*., 2015) and a recent study suggests that EDS5 which transports isochorismic acid from chloroplast into cytosol is also required for the Pip transportation from chloroplast to cytosol (Rekhter, *et al*., 2019b). These results give the evidence that the biosynthesis of Pip is occurred in chloroplast. Pip levels were substantially different in the local leaves of *ald1* and *sard4*

plants; whereas *ald1* plants were defective in Pip accumulation in both local and distal leaves, *sard4* plants were only defective in distal Pip accumulation. Thus, although ALD1 clearly regulates Pip biosynthesis, the precise role of SARD4 in Pip biosynthesis is unclear given that the *sard4* mutation does not abolish Pip biosynthesis in the infected leaves.

The study on the role of Pip in SAR has been largely linked to its ability to induce SA accumulation (Návarová *et al*., 2012). However, to deeply understand the mechanism underlying Pip-mediated SAR and its relation to other known chemical signals, I, collaborating with my colleagues conducted the experiment of SAR assay by exogenous application of Pip in different SAR defected mutant plants and metabolic analyses of SAR inducing chemicals. The results show that, Pip is a chemical inducer of SAR and functions primarily upstream of the NO-ROS-AzA-G3P branch of the SAR pathway. Moreover, like *sard4*, plants defective in the biosynthesis of ROS, AzA, G3P, or SA are defective in distal but not local Pip accumulation. I propose that the transport of SA and G3P to the distal tissue is important for Pip biosynthesis, where Pip in turn initiates the *de novo* synthesis of G3P. Together, these data establish the relationship between Pip and other structurally diverse chemical signals associated with SAR and highlight their coordinated function in the induction of SAR.

3.2 Results

3.2.1 Exogenous application of Pip confers SAR

An earlier study showed that whole plant application of Pip induces immunity in plants (Návarová *et al*., 2012). To test the requirement for Pip in SAR, I assayed its ability to induce immunity in distal untreated tissue when applied in a localized manner. For this, I pre-infiltrated WT plants (ecotype Col-0) with $MgCl_2$, *Pseudomonas syringae* pv. *tomato* (*Pst avrRpt2*), Pip (1000 µM), or methanol (negative control). The distal untreated leaves of all plants were then challenged with a virulent strain of *Pst* DC3000, and the growth of *Pst* DC3000 was monitored at 0- and 3-days post infiltration (dpi). Col-0 plants previously infected with *Pst avrRpt2* contained ~10- to 15-fold less *Pst* DC3000 compared to $MgCl_2$ pre-infiltrated plants (Fig. 3.1). Notably, pre-infiltration of Pip significantly reduced the growth of *Pst* DC3000 (Fig. 3.1), indicating that localized application of Pip induced systemic immunity. To confirm this finding, I assayed Pip-mediated SAR in the *ald1* mutant, which is defective in LAT activity and consequently unable to accumulate Pip (Fig. 3.2A & 3.2B). Local application of Pip was able to restore SAR in the *ald1* mutant (Fig. 3.2B), establishing that Pip is required for SAR.

To determine the optimal concentration of Pip required to yield a robust SAR, different concentrations (1 to 2000 µM) of Pip were applied on the local leaf respectively and infected the distal untreated leaves with *Pst* DC3000. SAR was strongest (as detected by a decrease in *Pst* DC3000 proliferation) in plants infiltrated with concentrations of 500 to 1000 µM Pip. However, higher concentrations (2000 µM) of Pip consistently induced significantly weaker SAR; SAR induced by 2000 µM Pip was comparable to that induced by 100 µM Pip. These data suggested that Pip induced SAR in a concentration-dependent manner and that 500 to 1000 µM Pip was an optimal concentration for the induction of SAR. To determine the time frame of Pip efficacy, SAR was assessed at different times

after treatment with 1000 µM Pip. Col-0 plants were infiltrated with Pip; their distal leaves were inoculated with *Pst* DC3000 at 6, 12, 24, or 48 hours after Pip infiltration; and *Pst* DC3000 growth was monitored at 0 and 3 dpi. As expected, Col-0 plants previously infected with *Pst avrRpt2* induced SAR compared to plants pre-infiltrated with $MgCl_2$ in their local leaves. The 24- and 48-hour time points produced a higher SAR compared to 6 and 12 hours, and the SAR was most effective after inoculation with the virulent pathogen was inoculated 48 hours after Pip application.
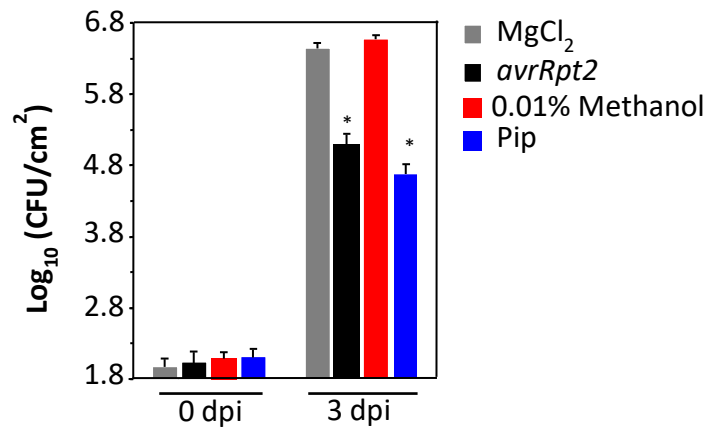
Fig. 3.1 Exogenous application of Pip confers SAR

SAR response in distal leaves of Col-0 plants treated locally with $MgCl_2$ solution (10 mM), methanol (0.01%), avirulent pathogen (*avrRpt2*), or Pip (1000 µM). The virulent pathogen (DC3000) was inoculated 48 hours after local treatments. Error bars indicate SD ($n = 4$). CFU, colony-forming units. Asterisks denote a significant difference with mock ($MgCl_2$ solution or methanol treated leaves, *t* test, $P < 0.05$). The experiment was repeated three times with similar results.
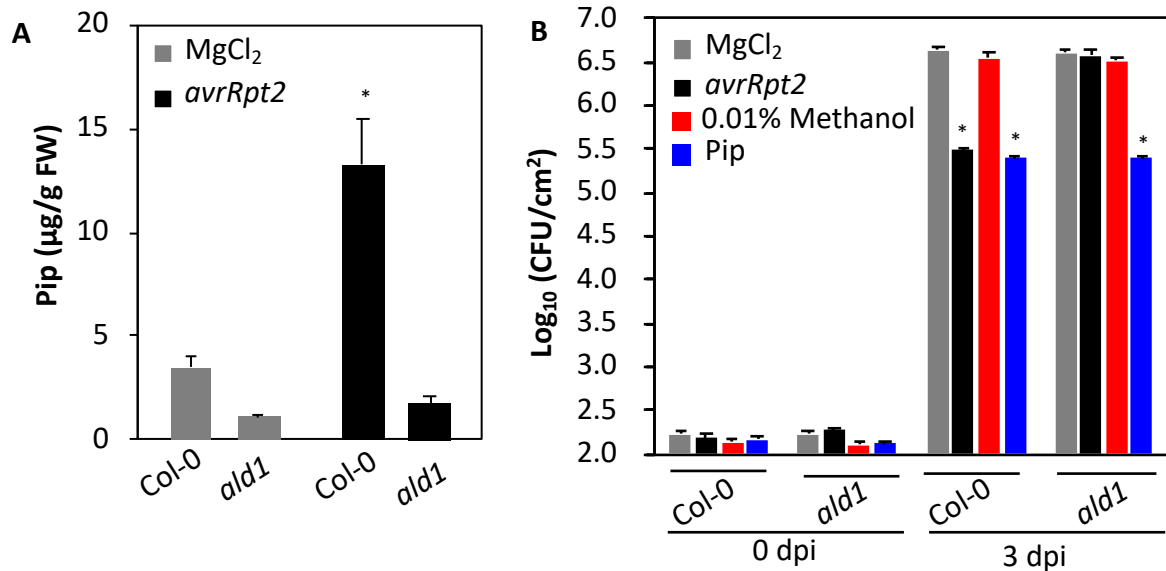
Fig. 3.2 Exogenous application of Pip restores SAR in Pip biosynthesis mutant plants
(A) Pip levels in local tissues of Col-0 and *ald1* plants after mock (10 mM $MgCl_2$ solution) and pathogen (*avrRpt2*) inoculations. The leaves were sampled 48 h post treatments. The error bars represent SD ($n = 4$). Asterisks denote a significant difference with mock (*t* test, $P < 0.05$). The experiment was repeated three times with similar results. **(B)** SAR response in distal leaves of Col-0 and *ald1* plants treated locally with $MgCl_2$ solution (10 mM), methanol (0.01%), avirulent pathogen (*avrRpt2*), or Pip (1000 μM). The virulent pathogen (DC3000) was inoculated 48 hours after local treatments. Error bars indicate SD ($n = 4$). Asterisks denote a significant difference with mock ($MgCl_2$ solution or methanol treated leaves, *t* test, $P < 0.05$). The experiment was repeated three times with similar results.

3.2.2 Pip functions upstream of NO, ROS, AzA, and G3P

To understand the molecular signaling pathway underlying Pip mediated SAR and its dependence on other SAR-associated signals, a transcriptome analysis of Pip-treated plants was conducted. Col-0 leaves treated with Pip showed an induction of 119 genes, of which 28 genes were shared between Pip- and *avr*-induced Col-0 plants. Likewise, 93 of 320 genes down regulated by Pip were shared between plants treated with Pip and *avr*. A survey of genes induced by Pip included several defense-associated genes including *PAD4*, *RBOHD*, *GRX*, and *AtNOA1*. Notably, *PR-1*, which is used as the marker gene for SA, was not induced by Pip (Fig 3.3) and this in turn was consistent with basal levels of SA in Pip-treated plants.
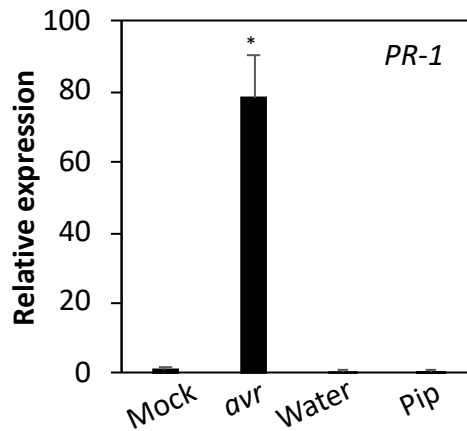
Fig. 3.3 Exogenous application of Pip is unable to induce *PR-1* gene expression
Real-time quantitative RT-PCR analysis showing relative expression levels of *PR-1* in plants treated with mock (10 mM $MgCl_2$ solution), avirluent pathogen (*avrRpt2*), water or 1000 μM Pip. Leaves were sampled 24 h post treatments for quantitative RT-PCR. The error bars indicate SD ($n = 3$). Asterisk denotes significant differences from mock treated leaves (*t* test, $P < 0.003$). Results are representative of two independent experiments.

Induction of *AtNOA1*, a gene that contributes to NO accumulation after avirulent pathogen infection (Wang *et al.*, 2014), suggested that Pip might be related to NO accumulation. To confirm, NOA1 protein level and NO levels analysis after Pip treatment were conducted. Both *avrRpt2* infection and Pip application induced NOA1 protein in local and distal leaves. The *avrRpt2* infection was unable to induce NOA1 protein in *ald1* plants, but the *ald1* plants induced WT-like levels of NOA1 after Pip application. An induction of NOA1 was associated with increased NO levels primarily in the chloroplasts of *avrRpt2* or Pip treated plants. As expected, Pip application did not induce NO in *noa1 nia2* plants. NIA2 is one of the two isoforms of nitrate reductase, which catalyzes NO production from nitrate. A mutation in NOA1 and either NIA1 or NIA2 abolishes avirulent pathogen-induced NO accumulation in Arabidopsis (Mandal *et al.*, 2012). Notably, consistent with previous results (Wang *et al.*, 2014), the distal leaves of Col-0 plants accumulated less NO compared to local leaves although these tissues accumulated similar levels of NOA1 protein. Like Col-0, the *ald1* plants accumulated NO after Pip application but not after *avrRpt2* infection. Together, these results suggested that Pip induces SAR by inducing NO accumulation and that depleted NO levels in *ald1* plants are associated with their inability to accumulate Pip. To confirm that Pip functioned upstream of NO, Pip was applied to *noa1 nia2* to assay the SAR impact of Pip in *noa1 nia2*, which is the mutant that do not accumulate NO in response to the avirulent pathogen (Wang *et al.*, 2014; Mandal *et al.*, 2012). Pip was unable to confer SAR on *noa1 nia2* plants, thus confirming that Pip-mediated SAR required NO.

The previous work in our lab showed that ROS, AzA and G3P operate downstream of NO in the SAR pathway. To test the involvement of these chemical signals in Pip-

mediated signaling, the levels of these metabolites after Pip treatment and Pip-mediated SAR in mutants that affected in ROS, AzA or G3P accumulation were tested. Exogenous treatment with Pip resulted in the accumulation of ROS in WT Col-0 plants, and this in turn was associated with increased cell death on Pip-treated leaves. Pip treatment did not induce ROS accumulation in the *rboh* mutant, which is defective in avirulent pathogen-induced ROS biosynthesis (Wang *et al*., 2014). ROS was measured using both quantitative assays and histochemical staining, and both assays showed similar results. The electron spin resonance (ESR) spectrometry-based quantitative analysis was carried out using α-(4-pyridyl N-oxide)-N-*tert*-butylnitrone (POBN), which detects hydroxyl and carbon-centered radicals. A time-course analysis for Pip-induced ROS accumulation showed that ROS levels increased within 6 hours after treatment. Pip treated plants did not show microscopic cell death at 6 hours after treatment, suggesting that Pip-induced ROS accumulation precedes cell death.

Consistent with the results with *noa1 nia2* plants, Pip was unable to confer SAR on *rbohD* or *rbohF* plants, both mutants of genes required for avirulent pathogen-induced ROS accumulation (Torres *et al*., 2002) and SAR (Wang *et al*., 2014). As predicted, Pip treatment also increased AzA levels but not in the *rbohD* mutant. Likewise, Pip treatment increased G3P levels, and exogenous Pip was unable to confer SAR on mutants defective in AzA biosynthesis (*mgd1*, *dgd1*, or *mgd1 dgd1* double mutant) or G3P (*gly1*, *gli1*, or *gly1 gli1* double mutant). Together, these results suggest that Pip-mediated SAR was dependent on the NO-ROS-AzA-G3P branch of the SAR pathway.

To reconfirm that Pip functions upstream of the NO-ROS-AzA-G3P branch of the SAR pathway, levels of various SAR-associated chemicals in *ald1* mutant plants, which

are compromised in Pip biosynthesis (Fig. 3.2A) were tested. I expected *ald1* plants to be compromised in ROS, AzA and G3P accumulation because these results suggested that Pip functions upstream of NO. Avirulent pathogen-inoculated *ald1* plants was unable to accumulate ROS, AzA, or G3P but did accumulate WT-like levels of SA. Consistent with their inability to accumulate ROS, the *ald1* plants showed reduced ion leakage (Fig 3.4), and this phenotype was reminiscent of the reduced ion leakage seen in *rboh* mutants (Torres *et al*., 2002). The *ald1* plants contained WT-like levels of C18 FAs and galactolipids that serve as precursors for AzA (Wang *et al*., 2014). This suggests that the reduced AzA levels in *ald1* plants were likely due to their inability to accumulate ROS rather than a defect in FAs or galactolipid levels. Consistent with this notion, localized application of ROS, AzA or G3P restored SAR in *ald1* plants, whereas exogenous SA did not. Unlike ROS, AzA and SA, G3P when applied by itself is a poor inducer of SAR because of the presence of phosphatases that can degrade G3P (Chanda *et al*., 2011). Together, these results strongly support a role for Pip upstream of the NO-ROS-AzA-G3P branch of the SAR pathway. This inferred upstream role is further correlated with the fact that Pip was unable to induce SAR in mutants impaired in SA biosynthesis (*sid2*) or signaling (*npr1* and *pad4*).
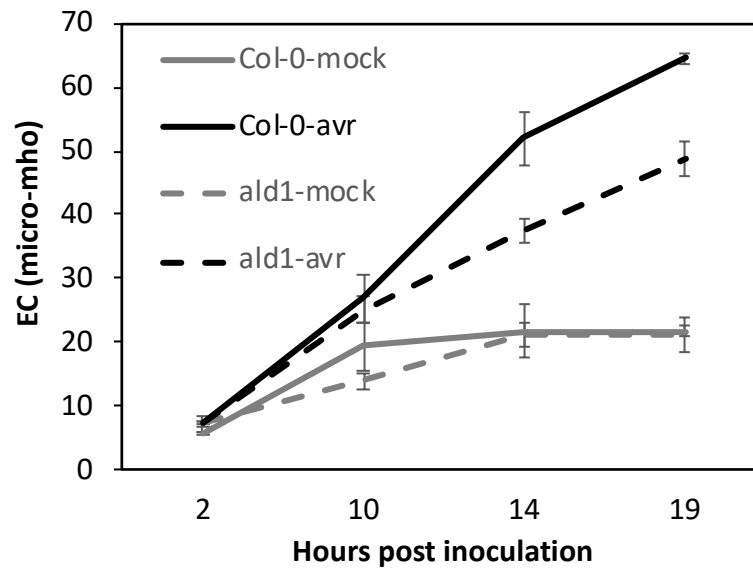
Fig. 3.4 *ald1* plants show reduced ion leakage

Electrolyte leakage in Col-0 and *ald1* plants infiltrated with $MgCl_2$ solution (10 mM) or *Pst avrRpt2*. Error bars represent SD (n = 6). This experiment was repeated twice with similar results.

I considered the possibility that Pip serves as a mobile signal during SAR because it functions upstream of NO. I tested whether impaired Pip biosynthesis affected SAR signal generation or perception. For this experiment, I collected petiole exudates (PEXs) from Col-0 (PEX-Col-0) and *ald1* (PEX-*ald1*) plants that were pre-infiltrated with either MgCl$_2$ (PEX$_{MgCl2}$) or *Pst avrRpt2* (PEX$_{avr}$). These were then infiltrated into a fresh set of Col-0 and *ald1* plants followed by inoculation of distal leaves with *Pst* DC3000 (Fig. 3.5A). The growth of *Pst* DC3000 was monitored at 0 and 3 dpi. The PEX$_{avr}$ from *ald1* conferred SAR on Col-0 plants but not on *ald1* plants. Likewise, the PEX$_{avr}$ from Col-0 plants induced SAR on Col-0 but not on *ald1* plants (Fig. 3.5A). Together, these data suggested that *ald1* plants can generate the SAR signal that functions upstream of Pip. PEX$_{avr}$ from *ald1* plants were able to induce Pip levels in Col-0 plants (Fig. 3.5B). Thus, Pip acts downstream of an unknown SAR signal.
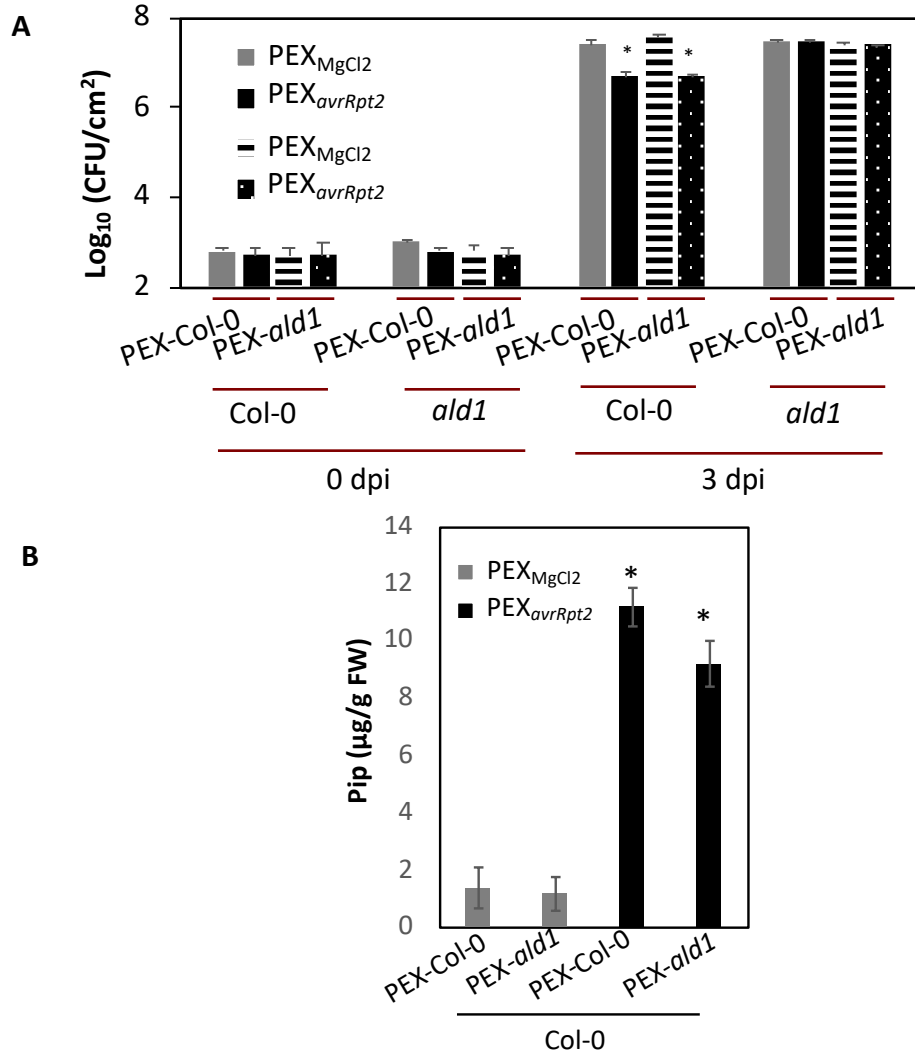
Fig. 3.5 *ald1* plants can generate SAR signal that functions upstream of Pip

(A) SAR response in Col-0 and *ald1* plants infiltrated with PEX collected from Col-0 or *ald1* plants that were treated either with $MgCl_2$ solution (PEX_{MgCl2}) or *avrRpt2* ($PEX_{avrRpt2}$). The distal leaves were inoculated with virulent pathogen at 48 hours after infiltration of primary leaves. Error bars indicates SD ($n = 4$). Asterisks denote a significant difference with mock (PEX_{MgCl2}) (*t* test, $P < 0.05$). The experiment was repeated twice with similar results. **(B)** Pip levels in Col-0 plants infiltrated with PEX collected from Col-0 or *ald1* plants that were treated either with 10 mM $MgCl_2$ solution (PEX_{MgCl2}) or *avrRpt2* ($PEX_{avrRpt2}$). Error bars indicate SD ($n = 4$). Asterisks denote a significant difference with mock (PEX_{MgCl2}) (*t* test, $P < 0.05$). The experiment was repeated twice with similar results.

3.2.3 Pip accumulation in distal tissues is dependent on SA and G3P

Quantification of Pip in plants inoculated with avirulent pathogens showed that Pip levels in infected leaves were ~2- to 3- fold higher compared to distal tissue (Fig. 3.6A). Furthermore, localized application of Pip also increased Pip levels in the distal tissue (Fig. 3.6A). To test whether Pip was mobile, I first assayed Pip in the distal leaves of Col-0 and *ald1* plants after localized application of Pip. The rationale was that any Pip accumulating in the distal tissue of *ald1* plants would represent Pip that was transported from the treated leaves because this mutant cannot synthesize Pip *de novo*. Distal leaves of *ald1* plants did accumulate Pip, although these levels were ~15-fold lower as compared to WT plants (Fig. 3.6B). The reduced distal accumulation of Pip in *ald1* plants was unlikely to be related to a defect in transport since localized Pip application rescued the SAR defect in these plants (Fig. 3.2B). Together, these results suggest that Pip is likely mobile and that transport of Pip to distal tissues is associated with its *de novo* synthesis. To test this possibility, I extracted Pip from PEX collected from 0.01% methanol-treated (PEX$_{mock}$) or Pip-treated (PEX$_{Pip}$) plants. The PEX$_{Pip}$ had higher levels of Pip than PEX$_{mock}$ (Fig. 3.6C), suggesting that Pip was indeed mobile. This result was also confirmed by thin-layer chromatography (TLC) analysis. To test it, 26 µM ^{14}C-labeled Pip was infiltrated into leaves of WT plants and Pip extracts from local and distal leaves were analyzed by thin-layer chromatography (TLC). The TLC analysis showed a band corresponding to ^{14}C-Pip in both local and distal leaves of mock- and *avrRpt2*-inoculated plants. This suggested that most of the ^{14}C-Pip was retained and transported as Pip or compounds structurally similar to Pip. The transport

assays also showed that *avrRpt2* infection promoted transport of Pip into distal tissue s by about 2-fold.
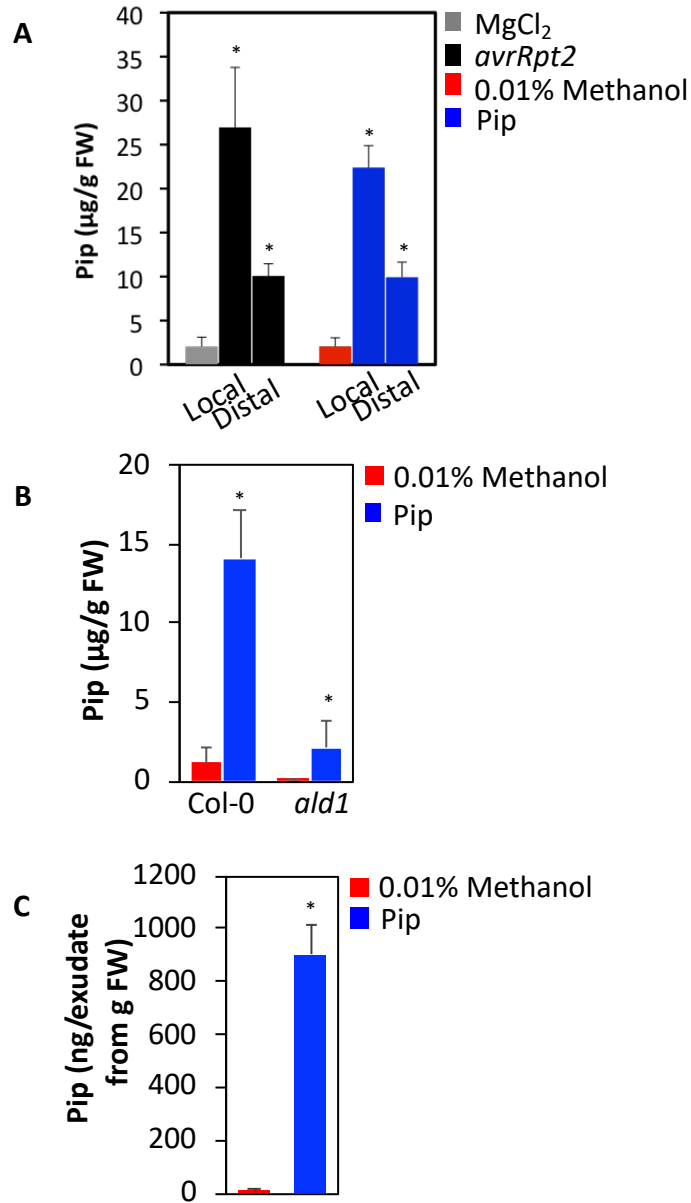
Fig. 3.6 Pip transports to systemic leaves

(A) Pip levels in local and distal tissues of Col-0 plants after mock (10 mM $MgCl_2$ solution) and pathogen (*avrRpt2*) inoculations or localized application of methanol (0.01%) or Pip (1000 μM). The leaves were sampled 48 hours after treatments. The error bars represent SD ($n = 4$). Asterisks denote a significant difference with mock (*t* test, $P <$

0.05). The experiment was repeated three times with similar results. **(B)** Pip levels in distal tissues of Col-0 and *ald1* plants after methanol (0.01%, mock)- and Pip (1000 μM)-infiltrations. The leaves were sampled 48 h post treatments. The error bars represent SD ($n = 4$). Asterisks denote a significant difference with mock (t test, $P < 0.05$). The experiment was repeated twice with similar results. **(C)** Pip levels in PEX collected from Col-0 plants after methanol (0.01%, mock) or Pip treatment. The infiltrated leaves (~2 g per sample) were sampled 48 hours after treatment. The error bars represent SD ($n = 4$). Asterisks denote a significant difference from mock treatment (t test, $P < 0.05$). The experiment was repeated twice with similar results.

Notably, Pip accumulation in local and distal leaves of Col-0 plants correlated with the induction of *ALD1* expression, although ALD1-derived Pip biosynthesis from lysine involves an additional intermediate step (Ding *et al*., 2016; Hartmann *et al*., 2017). Therefore, I tested whether *ALD1* overexpression could increase Pip levels by transiently overexpressing *ALD1-GFP* in *Nicotiana benthamiana* plants. As shown before (Cecchini *et al*., 2015), ALD1-GFP localized to the chloroplasts (Fig. 3.7A), and overexpression of *ALD1* increased Pip levels by ~400-fold (Fig. 3.7B). These data suggest that increased *ALD1* transcription results in Pip accumulation and that the intermediate steps following ALD1 activity are not rate-limiting for Pip biosynthesis.

Next, I assayed *ALD1* transcript and Pip levels in SAR-compromised mutants defective in the G3P branch of the SAR pathway. The *mgd1 dgd1* and *gly1 gli1* mutants expressed WT-like levels of *ALD1* gene expression in infected leaves but were unable to induce WT-like *ALD1* expression in the distal tissue (Fig. 3.8A & B). This further correlated with their Pip levels; *mgd1 dgd1* and *gly1 gli1* plants accumulated WT-like levels of Pip in infected but not in distal tissue. The ROS- and NO-defective *rboh* and *noa1 nia2* mutants, respectively, also accumulated WT-like levels of Pip in infected but not in distal tissue. Together, these results suggest that de novo synthesis of Pip in the distal leaves requires the functional NO-ROS-AZA-G3P branch of the SAR pathway.

A ALD1-GFP

B Pip (µg/g FW)

Empty vector 35S-ALD1-GFP
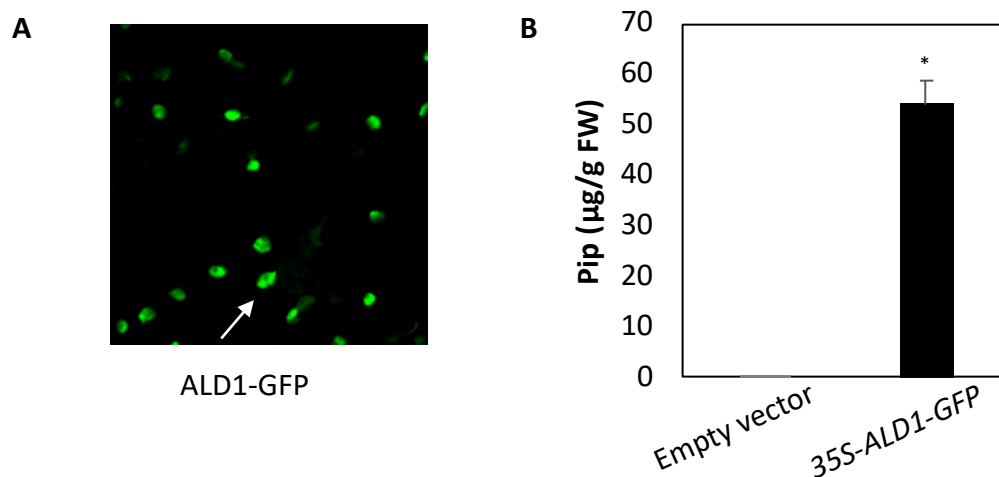
Fig. 3.7 Transient expression of *ALD1* increases the Pip level in *N. benthamiana*

(A) Confocal micrograph showing localization of ALD1-GFP transiently expressed in *N. benthamiana*. Agroinfiltration was used to express protein in *N. benthamiana* plants and arrow indicates chloroplast. **(B)** Pip levels in *N. benthamiana* plants transiently expressing *ALD1-GFP*. The leaves were sampled 48 h post agroinfiltration. The error bars represent SD ($n = 4$). Asterisks denote a significant difference with mock plants infiltrated with the empty vector (*t* test, $P < 0.05$). The experiment was repeated twice with similar results.
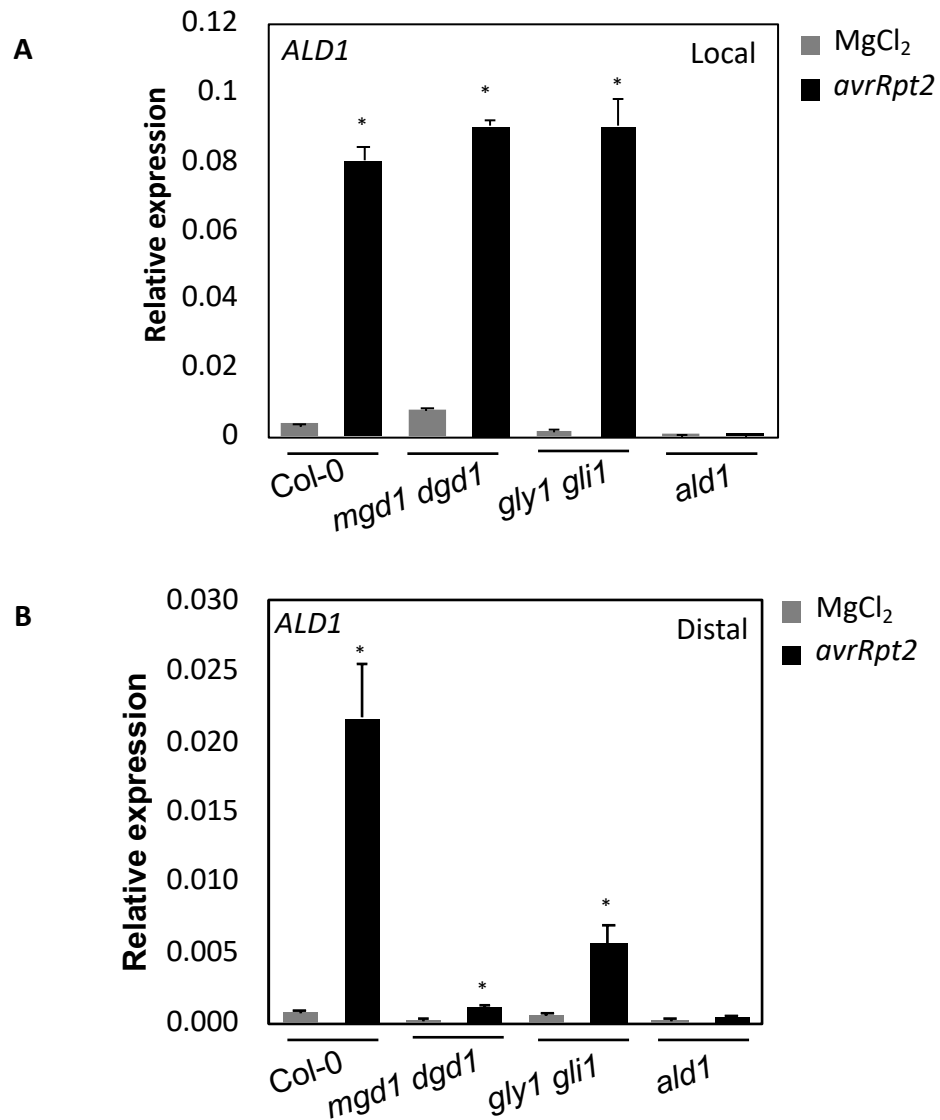
Fig. 3.8 Induction of Pip is associated with *ALD1* transcript levels

Realtime quantitative RT-PCR analysis showing relative expression levels of *ALD1* in local (left panel, **A**) or distal (right panel, **B**) of indicated genotypes treated with 10mM MgCl$_2$ solution (mock) or *avrRpt2*. Leaves were sampled 24 h post treatments. The error bars indicate SD ($n = 3$). Asterisk denotes significant differences from mock-treated leaves (*t* test, $P < 0.003$). Results are representative of two independent experiments.

Notably, the SA biosynthetic mutant *sid2* was also compromised in distal accumulation of both Pip and ROS (Fig. 3.9A & B) (Bernsdorff *et al.*, 2016). As expected, inoculated leaves or PEX from avirulent pathogen-infected *sid2* plants showed normal induction of G3P but not SA. These results suggest that in addition to G3P, avirulent pathogen-induced *de novo* synthesis of Pip in the distal leaves also requires SA. Consistent with a dual requirement for SA and G3P for SAR, SA treatment conferred SAR on *sid2* but not on *gly1 gli1* plants. Conversely, G3P did not confer SAR on *sid2* but was able to restore SAR in *mgd1 dgd1*, *gly1 gli1*, and *rbohD* plants. Moreover, local application of SA was associated with increased accumulation of Pip. Together, these results suggested that both G3P and SA were required for *de novo* synthesis of Pip in the distal leaves. However, these results did not explain why treatment with Pip was unable to restore SAR in *sid2* plants. To probe this question, Pip levels in distal tissues of *sid2* plants after localized application of Pip were tested. Unlike WT, the *sid2* plants did not accumulate Pip in their distal leaves. Likewise, *gly1 gli1* plants also showed impaired *de novo* synthesis of Pip in their distal leaves. Thus, I conclude that basal levels of SA and G3P are required for *de novo* synthesis of Pip in the distal tissues, a requirement that explains why localized application of Pip is unable to confer SAR on *sid2* plants.
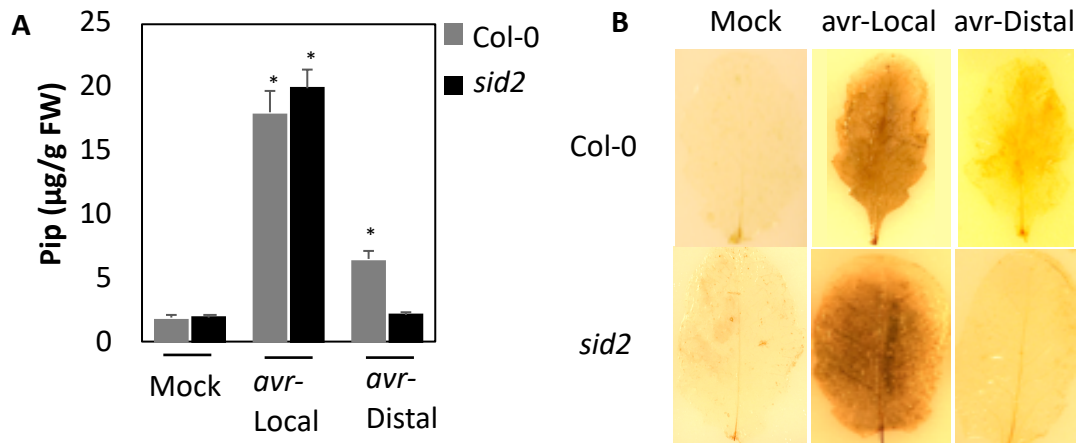
Fig. 3.9 Induction of Pip in the distal tissues is associated with SA

(A) Pip levels in local and distal tissues of Col-0 and *sid2* plants after mock (10 mM $MgCl_2$ solution) or pathogen (*avrRpt2*) inoculations. The leaves were samples 48 h post treatments. The error bars represent SD. Asterisks denote a significant different with mock (*t* test, $P < 0.05$). The experiment was repeated twice with similar results. **(B)** H_2O_2 levels in local and distal tissues of Col-0 and *sid2* plants after mock (10 mM $MgCl_2$ solution) or pathogen (*avrRpt2*) inoculations. The leaves were sampled 24 h post treatment and stained with DAB. The experiment was repeated twice with similar results.

3.3 Discussion

The finding that seemingly unrelated chemicals (NO, ROS, AzA, G3P, SA/MeSA, Pip, DA) function as SAR inducers led to the notion that SAR signaling involves multiple independent signals. However, the previous work in our lab established that NO, ROS, AzA, and G3P function in a linear pathway that functions in parallel with SA-derived signaling to induce SAR. Here, this work establish the relationship between Pip and the SA/ G3P-derived parallel signaling pathways and find that Pip functions upstream of the NO-ROS-AzA-G3P branch of SAR signaling and is consistent with a recent study that suggested a SA-independent function for Pip in SAR (Bernsdorff *et al*., 2016). Pip has been suggested to induce SA levels (Návarová *et al*., 2012). However, I show that Pip does not increase the expression of the SA marker *PR-1*; these data are in turn consistent with the finding of basal levels of SA in Pip-treated plants. These results suggest that Pip does not feed into the SA branch of the SAR pathway and primarily functions upstream of the NO-ROS-AzA-G3P branch of the SAR pathway. The placement of Pip in the NO-ROS-AzA-G3P branch is further supported by genetic and chemical analysis of mutants.

The Pip synthesis-deficient *ald1* mutant accumulates SA, but not ROS, AzA, or G3P, in response to infection with avirulent pathogen. Correspondingly, ROS, AzA, or G3P application induces SAR in *ald1* plants, but SA application does not. Furthermore, exogenous Pip cannot induce SAR on mutants impaired in pathogen-responsive biosynthesis/ accumulation of NO (*noa1 nia2*), ROS (*rbohD*/*rbohF*), AzA (*mgd1 dgd1*), and G3P (*gly1 gli1*). This lack of response indicates that Pip functions upstream of ROS in the NO-ROS-AzA-G3P branch of SAR signaling. Consistent with the dual requirement

for G3P- and SA-derived signaling for SAR, Pip is unable to induce SAR on mutants defective in SA biosynthesis (*sid2*). Likewise, NO and ROS, which serve downstream of Pip, are also unable to induce SAR on *sid2* (Wang *et al*., 2014).

Both SA and G3P contribute to avirulent pathogen-responsive Pip accumulation. Neither *sid2* (which contains low basal SA and is defective in pathogen-inducible SA accumulation) nor *gly1* (which is defective in pathogen-inducible G3P accumulation) mutants accumulate Pip in their distal tissue. However, this defect is not detected in the infected leaves of these mutants. One possibility is that Pip accumulation can be induced as long as threshold levels of either SA or G3P are achieved. Thus, the SA-defective *sid2* plants accumulate threshold levels of G3P (but not SA), while *gly1* plants accumulate threshold levels of SA (but not G3P) in their infected tissue, resulting in Pip accumulation. This is not the case in distal tissue, which does not accumulate nearly as much SA or G3P as infected tissue. Consistent with this notion, exogenous application of SA on *sid2* plants increases SA levels in the distal tissues as well as boosts Pip levels and is therefore able to confer SAR on *sid2* plants. On the other hand, exogenous Pip cannot confer SAR on *sid2* plants because these plants lack SA in their distal tissues, which is required for the *de novo* synthesis of Pip in the distal leaves. Like SA, G3P is also required for the de novo synthesis of Pip in distal tissue. Exogenous G3P was able to confer SAR on *ald1* plants, suggesting that increased levels of G3P override a requirement for Pip, as long as plants contain WT levels of SA.

On the basis of these results, I propose that Pip functions primarily upstream of the NO-ROS-AzA-G3P branch of the SAR pathway in infected tissue (Fig. 3.10). The Pip-induced SAR is dependent on the biosynthesis of downstream signals, and this explains

50

why Pip requires more time to confer effective SAR compared to downstream signals like G3P. Pathogen infection induces Pip accumulation in the infected tissue, which in turn induces the accumulation of NO, ROS, AzA and G3P. SA and G3P are transported to the distal leaves where they induce *de novo* Pip biosynthesis and thereby reactivate the NO, ROS, and AzA cascade culminating in the *de novo* biosynthesis of G3P. Notably, the absence of Pip does not alter the biosynthesis of SAR signals that act upstream of Pip. Clarifying the importance of Pip accumulation in infected versus distal tissues and elucidating how SA and G3P regulate Pip biosynthesis will yield further insights into the relationships between these various SAR signals.
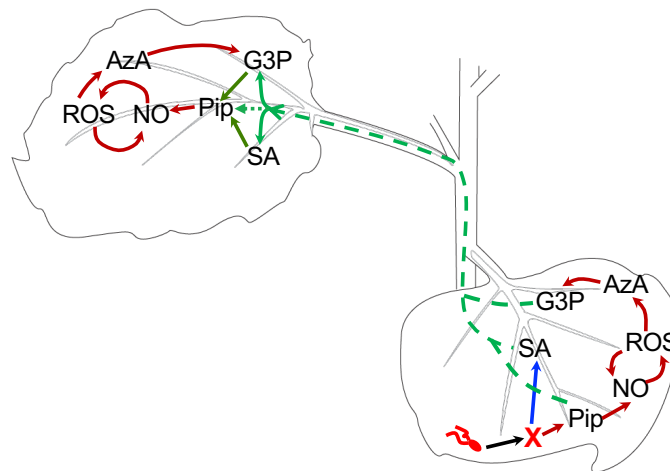
Fig. 3.10 A simplified model illustrating the relationship between SA, G3P, and Pip in local and distal leaves

Inoculation of avirulent pathogen triggers independent signaling events that lead to accumulation of SA and NO in the local leaves. NO triggers synthesis of ROS, which catalyze oxidation of free C18-unsaturated FAs that are released from membrane lipids. NO and ROS operate in a feedback loop. Oxidation of C18 FAs generates AzA, which triggers biosynthesis of G3P via up-regulation of genes encoding G3P biosynthetic enzymes. Of these, chemical signals SA, G3P, AzA, and Pip are detected in the PEX collected from leaves inoculated with avirulent pathogen. SA and G3P are required for

51

synthesis of Pip in the distal leaves. Exogenous G3P, but not SA, can overcome a requirement for Pip and confer SAR on *ald1* plants that are unable to synthesize Pip. Dashed green lines indicate transport of SA, G3P, and Pip from local to distal tissues.

CHAPTER 4

CHARACTERIZING THE ROLE OF FLAVIN-CONTAINING MONOOXYGENASE 1 (FMO1) AND SARCOSINE OXIDASE (SOX) IN SYSTEMIC IMMUNITY

4.1 Introduction

Flavin-containing monooxygenase (FMOs) were first discovered during the 1960s in hepatic microsomes which required NADPH and O_2 for its activity (Ziegler & Pettit, 1964). Later, FMOs have been found to be widely present in plants, microbes, and animals alike and are belong to a conserved group of enzymes catalyzing the oxygenation of substrates containing a nucleophilic nitrogen, sulfur, iodine, phosphorus, or selenium atom (Poulsen & Ziegler, 1995; Schlaich, 2007).

Arabidopsis plants contain 29 *FMO* genes, and among them, *FMO1* gene has an important role in plant immune response (Cao *et al*., 2019; Hansen *et al*., 2007; Li *et al*., 2008; Schlaich 2007; Olszak *et al*., 2006; Bartsch *et al*., 2006; Koch *et al*., 2006; Mishina & Zeier, 2006). The *FMO1* transcript level increases after virulent *Pst* DC3000 and avirulent *Pst avrRpm1* strain infection and the *fmo1* plants are more susceptible to *Pst* DC3000 than the WT plants and lack the ability to establish SAR (Bartsch *et al*., 2006; Mishina & Zeier, 2006).

In 2018, two different groups proposed that *FMO1* encodes a pipecolate hydroxylase which converts Pip into N-hydroxypipecolic acid (NHP) (Fig. 4.1) and localized leaf treatments or root applications restore pathogen resistance in *fmo1* plants as

well as in *ald1* plants (Hartmann *et al*., 2018; Chen *et al*., 2018). The difference in these two studies is that, unlike Hartmann *et al*. (2018), Chen *et al*. (2018) were unable to detect NHP in pathogen-infected plants. Instead, they found that NHP presented in infected Arabidopsis as the form of N-OGlc-Pip (Fig. 4.1), a conjugate formed by NHP and glucoside (Chen *et al*., 2018). However, Chen *et al*. (2018) detected NHP in transient assays when FMO1 was overexpressed in Pip-infiltrated *N. benthamiana* plants, thereby they assumed that NHP was possibly unstable and rapidly converted to N-OGlc-Pip via the activity of an unknown enzyme.
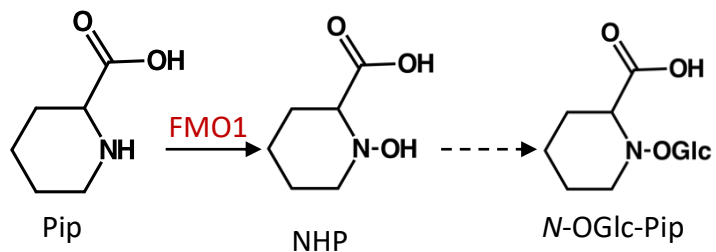
Fig. 4.1 Proposed Pip metabolism pathway via FMO1

FMO1 is proposed to catalyze Pip into NHP. Unknown enzymes are proposed to convert NHP into N-OGlc-Pip (Hartmann *et al*., 2018; Chen *et al*., 2018).

Another Pip metabolic enzyme, pipecolate oxidase (PIPOX), are widely found in mammals and microbes (Broquist, 1991). In human, Pip is oxidized into Δ^1-piperideine-6-carboxylate (P6C) via *Homo sapiens* PIPOX, which shares 33% identity with an Arabidopsis protein, sarcosine oxidase (SOX) (Goyer *et al*., 2004; Nishaki & Abe, 2015). The Pip level was elevated to 6-fold compared to WT plants when *SOX* expression was suppressed by RNA interference in Arabidopsis (Goyer *et al*., 2004), indicating that SOX functions in Pip metabolism. Goyer *et al*. (2004) proposed that SOX oxidizes Pip into P6C (Fig. 4.2), generating H_2O_2 as its byproduct via *in vitro* enzymatic assay.

The role of SOX and its bioproduct P6C in plant physiology, especially in plant immunity has not been studied yet. However, according to the function of SOX in catalyzing Pip into P6C, I assume that SOX might involve in plant immunity via affecting Pip metabolism thereby regulating Pip mediated plant immune response.
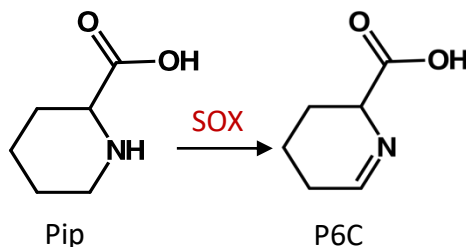
Fig. 4.2 Proposed Pip metabolism pathway via SOX
SOX is proposed to catalyze Pip into P6C. (Goyer *et al*., 2004).

In Chapter 3, I described that Pip confers SAR by regulating downstream SAR signals, as NO, ROS, AzA and G3P, however, the roles of Pip metabolic enzymes, FMO1 and SOX, and their products in SAR and the relation between Pip metabolic pathway and Pip mediated SAR pathway are not clear. To elucidate these questions, in this Chapter, I

conducted the experiment of SAR assay in the mutant lack of FMO1 or SOX function, respectively. I show that the FMO1 is required for SAR and its product NHP can induce SAR in WT plants. While the requirement of SOX in SAR is not conclusive since my results showed that plants mutant in *SOX* gene exhibited distinguishing SAR responses in different growth stages. However, *SOX* overexpression in WT plants impairs SAR and Pip accumulation after pathogen infection as well as Pip mediated SAR. In addition, optimal concentration of Pip is required to yield a robust SAR, so I propose that the function of SOX is to regulate Pip level remaining in optimal range, thereby regulate SAR response. Together, these data broaden our view that Pip metabolism is involved in SAR and open the door for us to understand the link between Pip metabolism pathway and SAR pathway.

4.2 Results

4.2.1 Exogenous application of NHP confers SAR and restores SAR on *ald1* and *fmo1*

Mishina & Zeier (2006) showed that *fmo1* was compromised in *Pst avrRpm1* induced SAR. To check that the loss of SAR ability in *fmo1* is not in a race-specific manner, I conducted the SAR assay with *Pst avrRpt2* and obtained the similar results that *fmo1* was compromised in *Pst avrRpt2*-mediated SAR (Fig. 4.3A). Hartmann *et al*. (2018) and Chen *et al*. (2018) provided evidence that irrigating NHP into the soil enhances the resistance in Col-0 (wild type), *ald1* and *fom1* plants. To test the requirement for NHP in SAR, local leaves were pre-infiltrated with $MgCl_2$ solution (10 mM, mock), *Pst avrRpt2* (10^7 CFU/mL), Pip (1000 μM), or NPH (1000 μM) in the Col-0, *ald1* and *fmo1* plants, the distal untreated leaves were then challenged with *Pst* DC3000 (10^5 CFU/mL), and the growth of *Pst* DC3000 was monitored at 0 and 3 dpi. Col-0 plants previously infiltrated with NPH (1000 μM) contained ~10-fold less *Pst* DC3000 compared to mock treated plants (Fig. 4.3B), indicating that localized application of NHP induced systemic immunity. In contrast to Pip, which only induces SAR in *ald1*, NHP induces SAR in both *ald1* and *fmo1*.
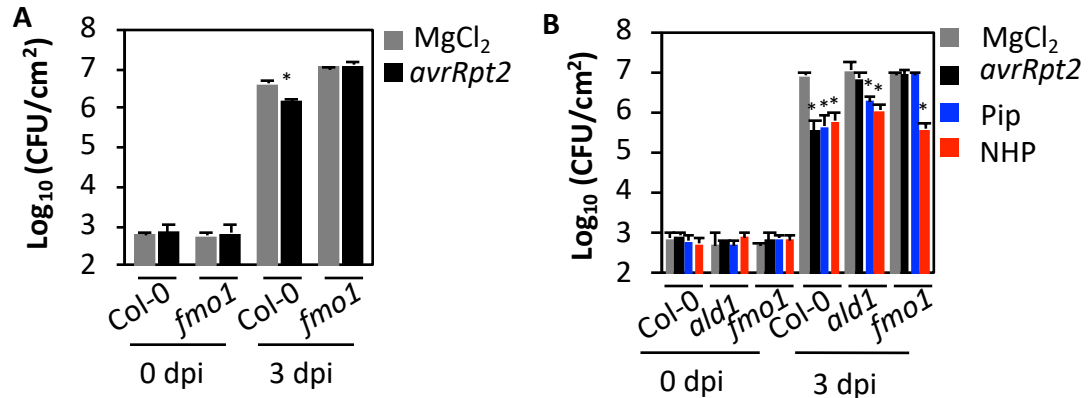
Fig. 4.3 Exogenous application of NHP confers SAR

(A) SAR response in distal leaves of Col-0 and *fmo1* plants treated locally with $MgCl_2$ solution, or avirulent pathogen (*avrRpt2*). The virulent pathogen (DC3000) was inoculated 48 hours after local treatments. Error bars indicate SD ($n = 4$). Asterisks denote a significant difference with mock (*t* test, $P < 0.05$). The experiment was repeated three times with similar results. **(B)** SAR response in distal leaves of Col-0, *ald1* and *fmo1* plants treated locally with $MgCl_2$, avirulent pathogen (*avrRpt2*), Pip (1000 μM) or NHP (1000 μM). The virulent pathogen (DC3000) was inoculated 48 hours after local treatments. Error bars indicate SD ($n = 4$). Asterisks denote a significant difference with mock (*t* test, $P < 0.05$). The experiment was repeated three with similar results.

4.2.2 Overexpression of *SOX* impairs SAR by reducing Pip accumulation

SOX is an enzyme which is proposed to catalyze conversion from Pip into P6C and H_2O_2 as well as sarcosine into glycine, formaldehyde and H_2O_2 (Goyer *et al*., 2004; Nishaki & Abe, 2015). Although it was named sarcosine oxidase, SOX exhibits higher enzymic activity on Pip than sarcosine (Goyer *et al*., 2004). Goyer *et al*. (2014) measured SOX activity based on the yield of the byproduct H_2O_2. To confirm that in the SOX enzymatic reaction, Pip is converted into others and characterize the product generated from Pip, I purified SOX protein from *E. coli* Rosetta (DE3) cells harboring pET28a-*SOX* (Fig. 4.4A) and quantified residual Pip levels after the enzymatic reactions. Pip level was largely reduced in the reaction mix within SOX protein compared with in the one without SOX (Fig. 4.4B). The product in the enzymatic reaction was confirmed as P6C via spectrophotometer and LC-MS analysis (data not shown). These data reconfirmed that the function of SOX in converting Pip into P6C.
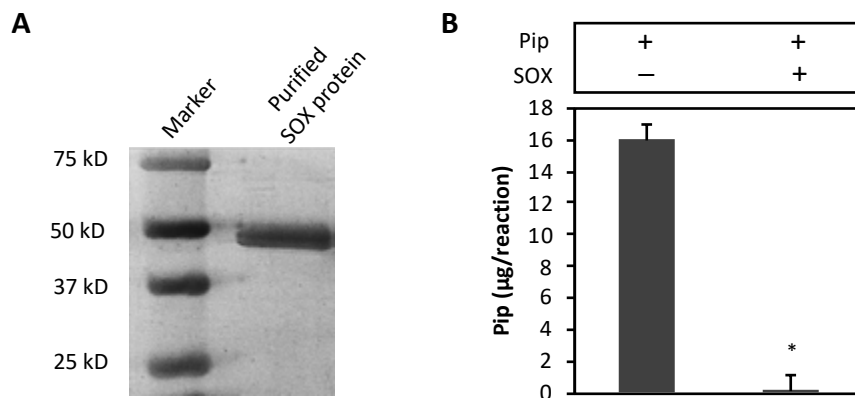
Fig. 4.4 Expression of *SOX* in *E. coli* and *in vitro* SOX enzymatic assay

(A) SDS-PAGE gel electrophoresis of soluble proteins of purified SOX protein. **(B)** Residual Pip levels after *in vitro* SOX enzymic reaction. The reaction was set up with 0.25μg purified SOX protein and 10 mM Pip adding water to reach 20 μL. The reaction without adding purified SOX protein was used as a control. The error bars represent SD (*n* = 4). Asterisks denote a significant difference with mock (*t* test, *P* < 0.05). The experiment was repeated twice with similar results.

To understand the function of *SOX* gene in SAR, I looked into *sox* mutant. I searched for *sox* mutant lines in the Arabidopsis seedstock databases, and selected two T-DNA insertion lines, Salk_017108 and GABI_680F04. Salk_017108 contains one T-DNA insertion in the promoter region of *SOX* while GABI_680F04 contains one T-DNA insertion in the coding sequence region (Fig. 4.5A). To find the knockout line, the homozygous plants of these two lines were detected with SOX antibody by western blot and GABI_680F04 was isolated as a knockout line for *SOX* (Fig. 4.5 B), so in this study, GABI_680F04 is referred to as *sox*. To characterize the SAR phenotype of *sox* plants, I tested two sets of plants of different ages for *Pst avrRpt2* mediated SAR, however, I obtained two distinguishing results. The younger *sox* plants which were five weeks after germination were compromised in SAR (Fig. 4.5C), and conversely, *sox* plants at the optimal growth stage which were six weeks after germination exhibited SAR (Fig. 4.5D). These results lead me to assume that SAR in *sox* mutant might be in an age dependent manner, however, to prove it, *sox* plants of more different ages are necessary to test for SAR in the further study, and it will be confirmed by my colleague.
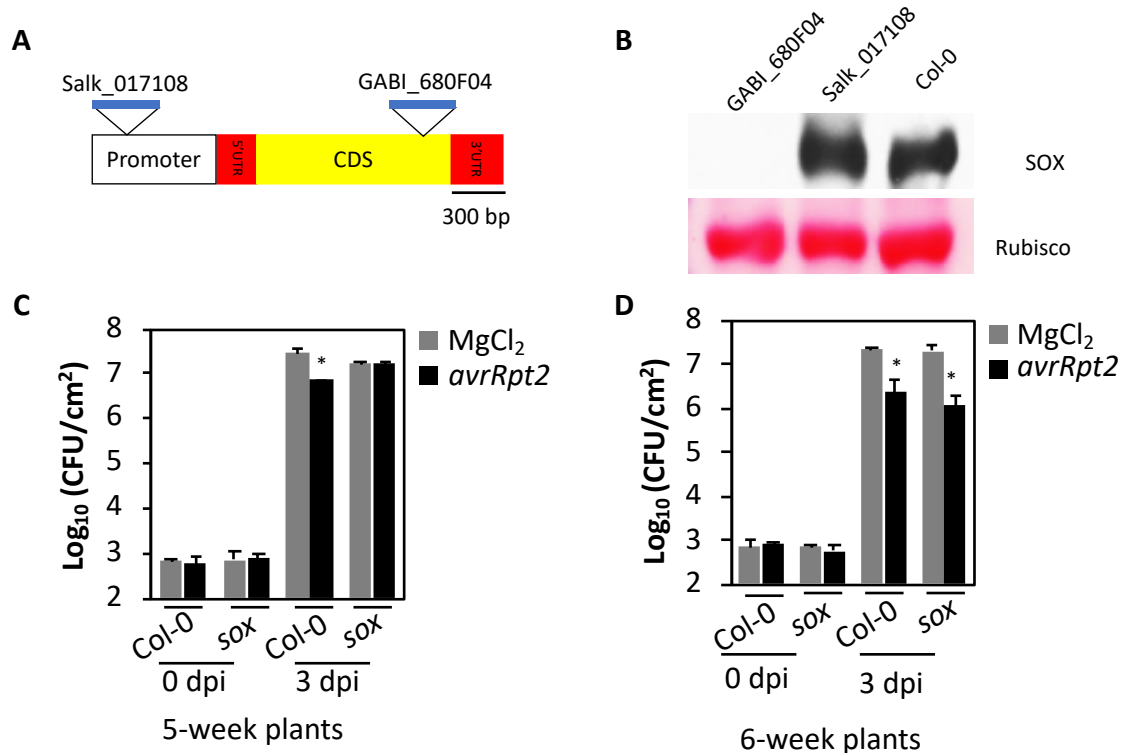
Fig. 4.5 Characterization of SAR phenotype of a *SOX* knock-out mutant

(A) Schematic representation of *SOX* gene. Triangles indicate the position of T-DNA insertion in the two alleles. UTR: untranslated region; CDS: coding sequence. **(B)** Protein immunoblot showing SOX levels in GABI_680F04, Salk_017108 and Col-0 plants. Ponceau S staining of the immunoblot was used as the loading control. The experiment was repeated four times with similar results. **(C)** SAR response in distal leaves of Col-0 and *sox* plants which were five weeks after germination treated locally with $MgCl_2$ solution (mock), avirulent pathogen (*avrRpt2*). The virulent pathogen (DC3000) was inoculated 48 hours after local treatments. Error bars indicate SD ($n = 4$). Asterisks denote a significant difference with mock (*t* test, $P < 0.05$). The experiment was repeated twice in a similar manner. **(D)** SAR response in distal leaves of Col-0 and *sox* plants which were six weeks after germination treated locally with 10 mM $MgCl_2$ solution (mock), avirulent pathogen (*avrRpt2*). The virulent pathogen (DC3000) was inoculated 48 hours after local treatments. Error bars indicate SD ($n = 4$). Asterisks denote a significant difference with mock (*t* test, $P < 0.05$). The experiment was repeated three times in a similar manner.

Another method to study the function of *SOX* gene in SAR is via generating transgenic plants which overexpress *SOX*. I transformed *A. tumefaciens* with pGWB5-*SOX* plasmid which contains *35S-SOX-GFP* gene fragment into Col-0 via floral dip method (Clough & Bent, 1998) and obtained 17 lines of *35S-SOX-GFP*:: Col-0 transgenic plants. Among these lines, #2 and #17 lines shows strong green fluorescence by confocal microscope assay. The confocal microscope assay showed SOX-GFP localized in the cytosol and nucleus (Fig. 4.6A). Arabidopsis SOX was proposed to localize in peroxisomes to carry out its enzymatic function (Goyer *et al*., 2004) so it is easy to understand why SOX localized in the cytosol since peroxisomes widely distribute in cytosol. However, it is not clear to explain the function of nuclear localization of SOX by the data I have until now. Post translational modification (PTM) of a protein, such as phosphorylation, ubiquitination, or others, can change the localization of the protein and then activate or inactivate protein function and the most classic model is NPR1 (Withers & Dong, 2016). So, I assume that SOX can be modified and then re-localized into nucleus to remain hibernating or for degradation. To solve this question, mutant SOX proteins which have one subcellular localization will be utilized in the further study.

I tested *avrRpt2* mediated SAR in these two transgenic lines and they both showed compromised SAR (Fig. 4.6B). Since SOX metabolizes Pip *in vitro*, I assumed that overexpressed SOX protein might continually convert Pip into P6C *in planta* thereby affect Pip accumulation upon pathogen infection which results in compromised SAR.
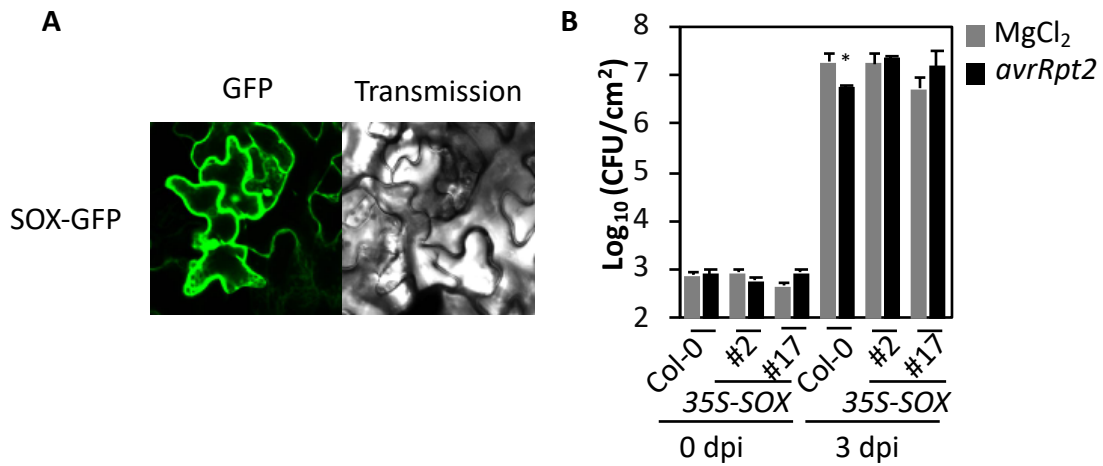
Fig. 4.6 Overexpression of *SOX* compromises SAR

(A) Confocal micrograph showing localization of SOX. **(B)** SAR response in distal leaves of Col-0 and *35S-SOX-GFP* transgenic plants treated locally with $MgCl_2$ solution or avirulent pathogen (*avrRpt2*). The virulent pathogen (DC3000) was inoculated 48 hours after local treatments. Error bars indicate SD ($n = 4$). Asterisk denotes significant differences from methanol treated leaves (*t* test, $P < 0.05$).

To test it, Pip level was quantified after infiltrating with *Pst avrRpt2* in Col-0 and *35S-SOX* (in this chapter, *35S-SOX* is referred to as #17 line) plants. Both basal and induced levels of Pip were reduced in *35S-SOX* plants compared with WT Col-0 (Fig. 4.7A), indicating that *35S-SOX* plants failed to accumulate Pip whether suffering pathogen challenge or not. According to this result, there are two possible reasons to explain why *35S-SOX* plants is unable to accumulate Pip: 1) Pip is degraded by SOX in *35S-SOX* plants due to the overexpression of SOX; and 2) overexpression of *SOX* affects endogenous Pip biosynthesis, because Pip biosynthesis mutant, *ald1*(Fig. 4.7B), is also unable to accumulate Pip. To explain it, I quantified Pip levels in *35S-SOX* plants pre-infiltrated with Pip and found that the Pip level in the infiltrated leaves of *35S-SOX* plant were much lower than in Col-0 (Fig. 4.7C), which were distinguishing with the results in *ald1* plants (Fig. 4.7D), since *ald1* plants contained similar level of Pip with Col-0 after infiltrating with Pip. These results suggested that Pip is degraded by SOX in *35S-SOX* plants. In addition, an increased level of P6C was detected in *35-SOX* plants after *Pst avrRpt2* infection or Pip infiltration by LC-MS (data not shown), suggesting that Pip level is induced by *avrRpt2* but once Pip is synthesized, it is degraded into P6C, so that*35S-SOX* plants failed to accumulate Pip after pathogen infection thereby, was unable to generate SAR.
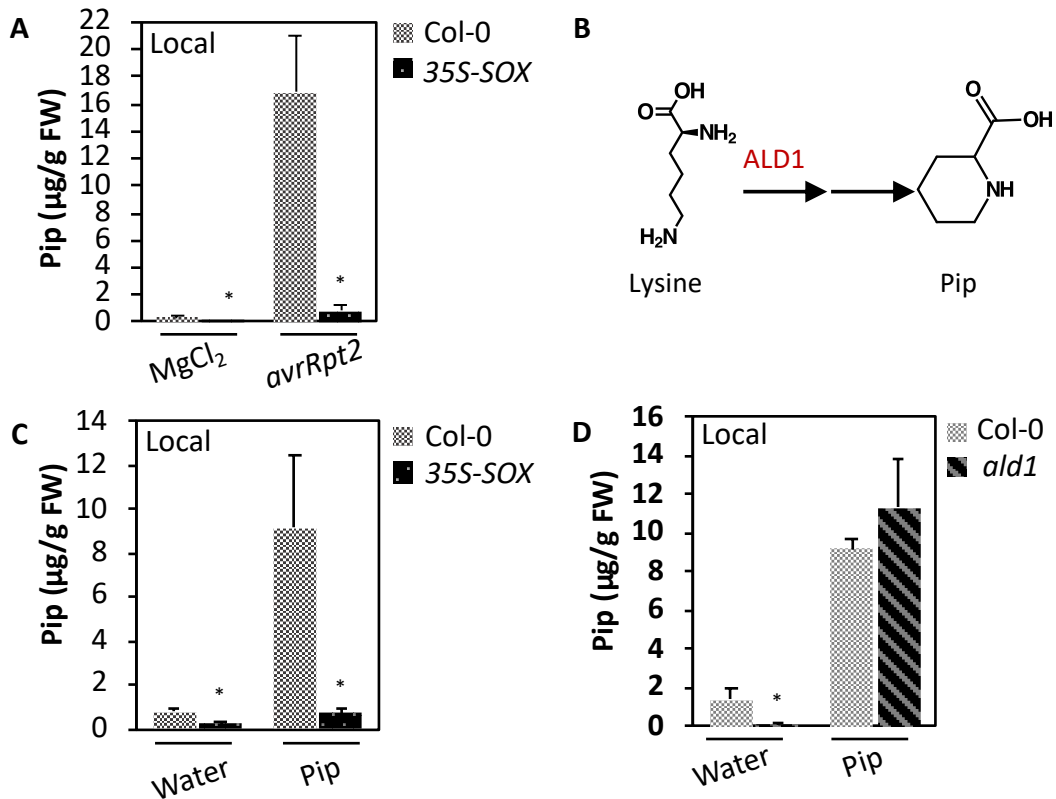
Fig. 4.7 Overexpressing *SOX* in Col-0 reduces Pip accumulation

(A) Pip levels in local tissues of Col-0 and *35S-SOX* plants after mock (10 mM $MgCl_2$) and pathogen (*avrRpt2*) inoculations. The leaves were sampled 48 hours after treatments. The error bars represent SD ($n = 4$). Asterisks denote a significant difference between Col-0 and *35S-SOX* plants (*t* test, $P < 0.05$). This experiment was repeated three times with similar results. **(B)** Schematic representation of Pip biosynthesis pathway. **(C, D)** Pip levels in local tissues of Col-0, *35S-SOX* (C) or *ald1* (D) plants after water- and Pip (1000 µM)-infiltrations. The leaves were sampled 48 h post treatments. The error bars represent SD ($n = 4$). Asterisks denote a significant difference between Col-0 and *35S-SOX* plants (*t* test, $P < 0.05$). This experiment was repeated twice with similar results.

Besides overexpression of *SOX* compromised *Pst avrRpt2* induced SAR, it also compromised Pip meditated SAR (Fig. 4.8A) which is more likely due to the depletion of Pip in *35S-SOX* plants (Fig. 4.7C). In Chapter 3, I described that G3P serves as signal in downstream Pip in SAR pathway which is able to restore SAR in Pip deficient mutant, *ald1*. To test the capability of G3P to restore SAR in *35S-SOX* plants, G3P induced SAR assay was carried out in Col-0 and *35-SOX* plants. However, unlike in *ald1* plants, G3P was unable to restore SAR in *35S-SOX* plants (Fig. 4.8B). Notably, although both *ald1* and *35S-SOX* plants contain reduced level of Pip compared with Col-0 plants with or without *Pst avrRpt2* challenge, *35S-SOX* plants accumulate increased level of P6C (data not shown) upon *Pst avrRpt2* infection. Together, these results indicate that overexpression of SOX and its product, P6C might interfere with SAR pathway that is downstream Pip.
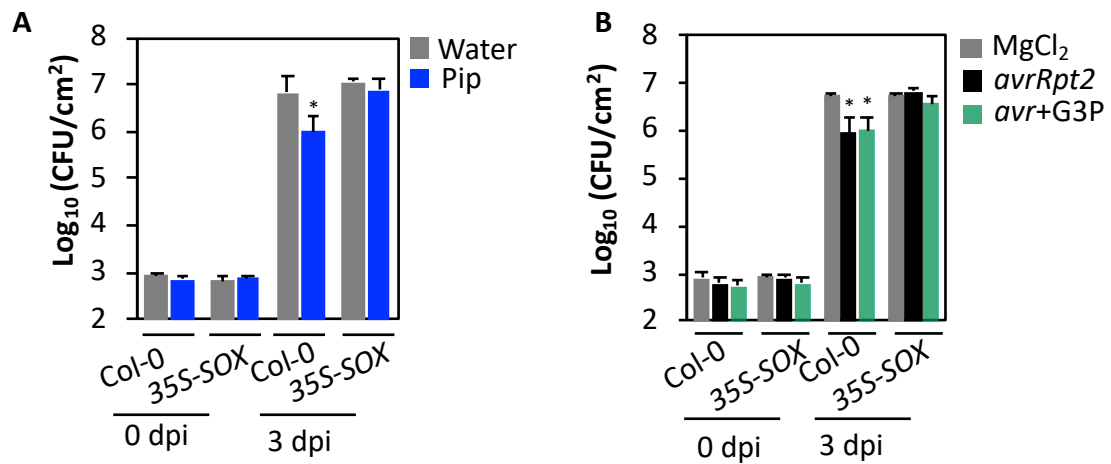
Fig. 4.8 Overexpression of *SOX* compromises Pip mediated SAR

(A, B) SAR response in distal leaves of Col-0 and *35S-SOX* plants treated locally with water or Pip (1000 μM) (A) and $MgCl_2$ solution, avirulent pathogen (*avrRpt2*) or G3P(100μM) plus *avrRpt2* (B). The virulent pathogen (DC3000) was inoculated 48 hours after local treatments. Error bars indicate SD (*n* = 4). Asterisk denotes significant differences from water or $MgCl_2$ treated leaves (*t* test, *P* < 0.005). This experiment was repeated twice with similar results.

4.3 Discussion

In this chapter, I characterized the function of FMO1 and SOX in SAR. Both FMO1 and SOX metabolize Pip, but their importance for SAR are different. FMO1 is essential for SAR since the knockout mutant *fmo1* is defective in SAR (Fig. 4.3A) and its product, NHP confers SAR (Hartmann *et al*., 2018), while the function of SOX in SAR is not conclusive because although 5 week-age *sox* plants were SAR compromised, 6 week-age *sox* plants which is at its optimal growth stage exhibited normal SAR.

In Chapter 3, I have described that Pip mediated SAR is concentration dependent, Pip of too low or too high concentration failed to give SAR in Col-0 plants. So, I assume that the function of SOX in SAR is to maintain Pip level in an optimal range, and thereby, once *SOX* is mutated in plants, Pip level is unregulated during different plant growth stages, resulting different SAR responses. To confirm, SAR assay in *sox* mutant of different growth stages and Pip level in the corresponding growth stages need to be included in the further study.

Three signaling pathways are regulated by or derived from Pip: Pip-NO/ROS-AzA-G3P pathway, FMO1-mediated Pip-NHP pathway and SOX-mediated Pip-P6C pathway. I have described in Chapter 3 and this chapter, both Pip-NO/ROS-AzA-G3P and Pip-NHP pathway contribute to SAR, but the relation between these two pathways is not elucidated. Further study in quantification of NO, ROS, AzA and G3P in plants infiltrated with NHP, NHP induced SAR assay in the mutant defective in NO, ROS, AzA and G3P and other experiments, will be included to explain this question.

On the basis of my results, I propose Pip-P6C pathway might have a negative impact on SAR since the *35S-SOX* plants accumulate high P6C after *Pst avrRpt2* inoculation but still compromised in SAR (Fig. 4.6B). And G3P, operating downstream of Pip in the SAR pathway, failed to restore SAR (Fig. 4.8B) in the *35S-SOX* plants indicating that P6C might inhibit Pip-NO/ROS-AzA-G3P pathway. To clarify the impact of P6C in SAR, SAR assay mediated by purified P6C are more convincing and further insights will focus on elucidating the relationship between P6C, NHP and other SAR related chemicals.

CHAPTER 5

CHARACTERIZING THE ROLE OF ASCORBIC ACID AND ASCORBATE PEROXIDASE IN SYSTEMIC IMMUNITY

5.1 Introduction

L-ascorbic acid (AsA) is a common name for the six-carbon sugar derivative L-threohex-2-enono-1,4-lactone. It has important antioxidant and metabolic functions in both plants and animals. However, AsA is not synthesized in the human body and must be taken in through diet, so it is also known as 'vitamin C'. Not only humans, and some other animal species lack the capacity to produce AsA, so plant derived AsA is the major source of vitamin C in the human diet. AsA is also an essential compound for plants with important roles as an antioxidant to protect plant cell against ROS from photosynthetic and respiratory process.

Based on biochemical evidence, Wheeler *et al*., (1998) described the first AsA biosynthetic pathway in plants. In this pathway, the D-glucose is converted into AsA through the following intermediates: GDP-D-mannose, GDP-L-galactose, L-Galactose-1-phosphate, L-Galactose, and L-Galactono-1,4-lactone. This pathway is named the D-Mannose 1-phosphate pathway, L-Galactose pathway or Smirnoff-Wheeler pathway (Fig. 5.1). Several alternative pathways were also found in different plant species and they are named after their primary metabolites, respectively: D-Galacturonate (Agius *et al*., 2003), L-Gulose (Wolucka & Van Montagu, 2003) and *myo*-Inositol (Lorence *et al*., 2004). However, the main pathway in Arabidopsis is the D-Mannose 1-phosphate pathway.
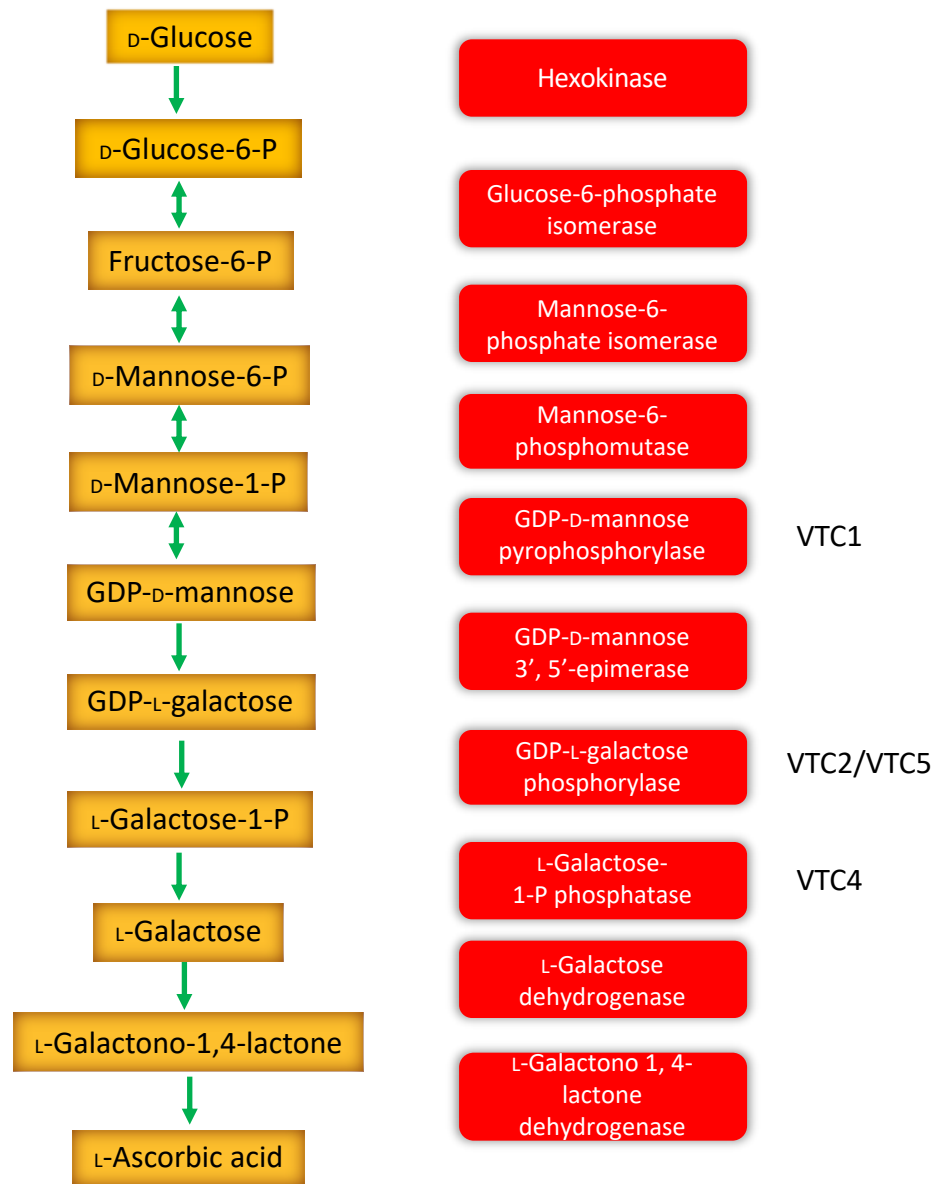
Fig. 5.1 A simplified scheme showing components of Smirnoff- Wheeler pathway
Content in yellow rectangle: name of intermediate metabolite in Smirnoff- Wheeler pathway; content in the red rectangle: name of enzyme of the step (alternative name of several enzymes was labeled on the right); green arrow was utilized to show the direction of reaction.

Four Arabidopsis mutants that were first identified in a screen for mutants with increased ozone-sensitivity were then characterized as lacking AsA (Conklin *et al.*, 1996; Conklin *et al.*, 2000). Due to their low level of AsA (vitamin C), the mutated genes were named *VTC1*, *VTC2*, *VTC3*, and *VTC4*. Characterization of the *vtc1* (Conklin *et al.*, 1999), *vtc2* (Linster *et al.*, 2007) and *vtc4* (Conklin *et al.*, 2006) mutants, have allowed the identification of three of the enzymes required for AsA synthesis through the Smirnoff-Wheeler pathway. *VTC1*, *VTC2* and *VTC4* encode GDP-D-mannose pyrophosphorylase (Conklin *et al.*, 1999), GDP-L-galactose phosphorylase (Linster *et al.*, 2007) and L-Galactose-1-P phosphatase (Conklin *et al.*, 2006), respectively. The function of VTC3 genes has not yet been elucidated. However, *VTC5* gene was characterized as encoding GDP-L-galactose phosphorylase and shows most similarity with *VTC2*, which means the two paralogous genes *VTC2* and *VTC5* function in conversion from GDP-L-galactose to L-galactose-1-phosphatase (Linster & Clarke, 2008). The EMS mutant, *vtc1-1,* containing only 25% AsA content compared to WT plants (Conklin *et al.*, 1999), and show elevated resistance to virulent pathogens, which suggests that ascorbate deficiency is associated with immune resistance (Barth *et al.*, 2004).

To detoxify and regulate the cellular levels of ROS, AsA reacts with H_2O_2 by the catalysis of ascorbate peroxidases (APXs). APX catalyzes AsA oxidation to dehydroascorbate by electron transfer from AsA to H_2O_2, consequently reducing H_2O_2 to water (Caverzan *et al.*, 2012). APXs have been widely found in vascular plants and is distributed in different cell compartments including cytosol, chloroplasts, peroxisomes, and mitochondria (Shigeoka *et al.*, 2002). In Arabidopsis, eight APX isoforms have been found in different subcellular locations. Among these eight APXs, APX1 is localized in

the cytosol, s-APX in the chloroplast stroma and t-APX in in the chloroplast thylakoids (Caverzan *et al*., 2012). Plants which lose function of APXs exhibit increased sensitivity to H_2O_2, which is an important ROS related biotic and abiotic stresses (Caverzan *et al*., 2012).

In this study, I examined the involvement of AsA biosynthesis proteins and three different localized APXs in SAR. I found that the AsA-deficient mutant, *vtc1*, is impaired in SAR, and high local resistance including PTI and ETI. The high local resistance is proposed to be associated with high level SA and Pip in *vtc1* plants. I also show that cytosol localized protein APX1 and stroma localized protein s-APX are involved in SAR and exogenous application of Pip restored SAR in *apx1* and *s-apx* mutants. Together, my study provides additional support for the interaction between Pip and ROS during SAR.

5.2 Results

5.2.1 Mutants containing low level of AsA are compromised in SAR

An earlier study showed that mutants *vtc1* and *vtc2* contain about 25% of the wild-type level of total AsA (Conklin *et al*., 2000). To test if AsA deficiency affects SAR, I assayed SAR in WT and *vtc1* plants. However, unlike Col-0 (WT) plants, the pre-infiltration of *Pst avrRpt2* in *vtc1* mutant plants did not reduced the growth of *Pst* DC3000 compared with mock inoculation (Fig. 5.2A), indicating that the *vtc1* mutant plants impaired SAR. To further test if the impaired SAR phenotype in *vtc1* is due to its low level of AsA but not the accumulation of D-Mannose-1-phosphate, the substrate of VTC1 (converting D-Mannose-1-phosphate into GDP-D-mannose), I assayed *Pst avrRpt2*-mediated SAR in another AsA-deficient mutant, *vtc2* (VTC2 converts GDP-L-galactose into L-Galactose-1-phosphate). Notably, *vtc2* is also compromised in SAR (Fig. 5.2B). Together, these data suggest that AsA deficiency impairs the establishment of SAR.
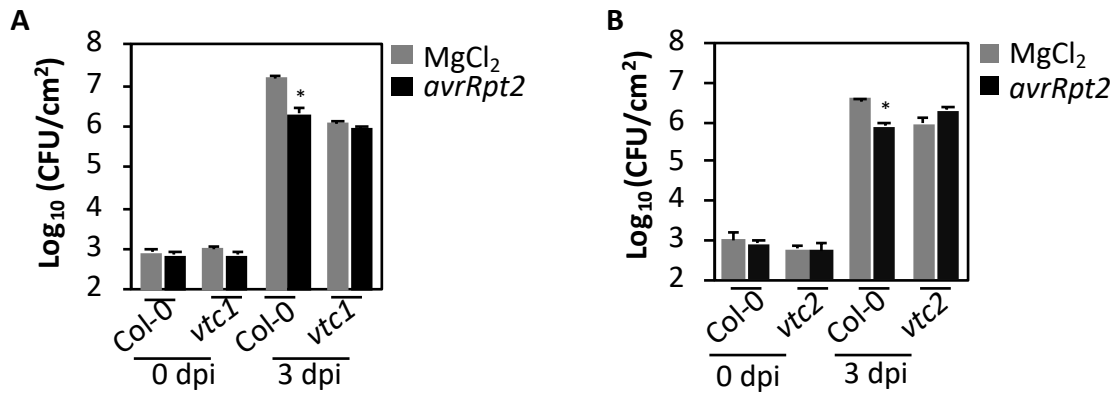
Fig. 5.2 AsA-deficient mutants are compromised in SAR

(A, B) SAR response in Col-0, *vtc1* (A) and *vtc2* (B) plants infiltrated with 10 mM MgCl$_2$ solution (mock) or *avrRpt2*. The distal leaves were inoculated with the virulent pathogen at 48 hours after infiltration of primary leaves. Error bars indicates SD ($n = 4$). Asterisks denote a significant difference with mock (t test, $P < 0.05$). The experiment was repeated three times with similar results.

Barth *et al*. (2004) shows that AsA-deficiency in *vtc1* results in its resistance to virulent *Pst* and *Peronospora parasitica,* an oomycete pathogen causing downy mildew (Koch & Slusarenko, 1990). Here, in SAR assays of *vtc1*, there is significantly different growth of *Pst* DC3000 between Col-0 and *vtc1* plants in the mock treatment. To determine if *vtc1* plants are resistant to avirulent pathogen *Pst avrRpt2* and reconfirm the enhanced resistance to virulent *Pst* DC3000 of *vtc1*, I challenged Col-0 and *vtc1* plants with *Pst avrRpt2* and *Pst* DC3000, respectively, and measured the bacterial growth at 0 dpi and 3 dpi. The *vtc1* plants contained ~10- fold less *Pst avrRpt2* and *Pst* DC3000 compared to the Col-0 plants (Fig. 5.3A & B), indicating that *vtc1* is resistant to both avirulent and virulent pathogens. Notably, the transcript level of *PR-1,* the marker gene for SA signaling, (Fig. 5.3C) and *ALD1,* the marker gene for Pip biosynthesis (Fig. 5.3D) were higher in *vtc1* than in Col-0 plants*,* as well as SA and Pip level were also higher in *vtc1* than in Col-0 plants (Fig. 5.3E & F). These data suggested that the enhanced resistance in *vtc1* is associated with the accumulation of SA and Pip.

To understand the function of VTC1 in the SAR pathway, I exanimated various SAR-associated chemicals in the *vtc1* mutant. However, localized application of SA, Pip, DETA (NO donor), ROS and G3P failed to confer or fully confer SAR in *vtc1* plants (Fig. 5.4A-E). I consider if this might be because *vtc1* plants exhibit high resistance and is already primed for pathogen infection, so *vtc1* plants lack spare capability to increase their resistance. However, foliar spraying and root irrigating SA onto whole *vtc1* plants enhanced their resistance to virulent *Pst* DC3000 (Fig. 5.4F). So, the former explanation is untenable. The compromised SAR phenotype in *vtc1* plants might instead be due to the incapability of signal transportation or signal amplification in the distal tissues.
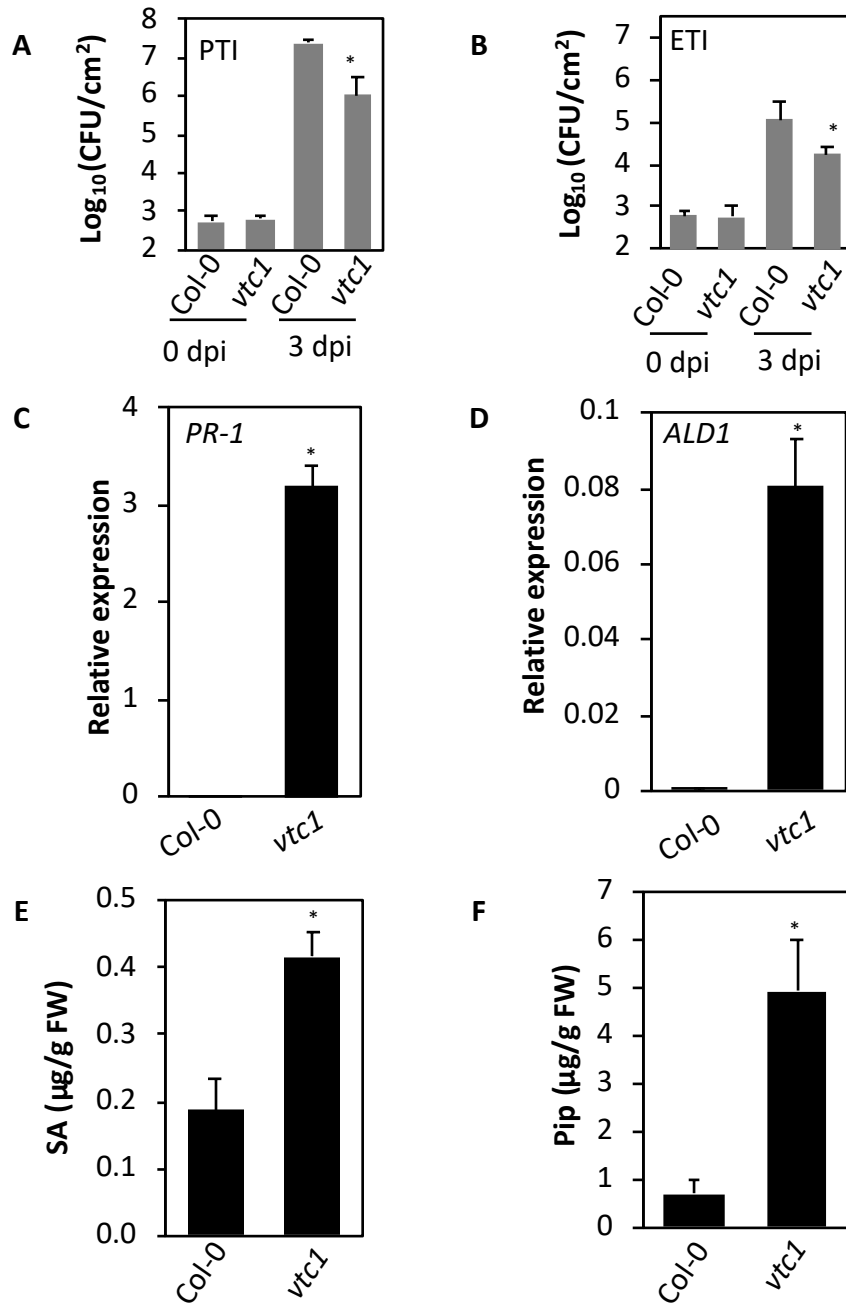
Fig. 5.3 Increased resistance in *vtc1* mutant is dependent on its high level of SA and Pip

(A, B) Responses of the Col-0 and *vtc1* plants upon infection with the virulent pathogen (*Pst* DC3000 (A) and avirulent pathogen (*Pst avrRpt2*) (B). The error bars represent SD (*n* = 4). Asterisks denote a significant difference with Col-0 (*t* test, $P < 0.05$). The experiment was repeated three times with similar results **(C, D)** Real-time quantitative RT-PCR analysis showing relative expression levels of *PR-1* (C) and *ALD1* (D) in Col-0 and *vtc1*

plants. The error bars indicate SD ($n = 3$). Asterisk denotes significant differences from Col-0(t test, $P < 0.003$). Results are representative of two independent experiments. **(E, F)** SA levels (E) and Pip levels (F) in local tissues of Col-0 and *vtc1* plants after mock (10 mM $MgCl_2$ solution) and pathogen (*avrRpt2*) inoculations. The leaves were sampled 48 hours after treatments. The error bars represent SD ($n = 4$). Asterisks denote a significant difference with mock (t test, $P < 0.05$). The experiment was repeated twice with similar results
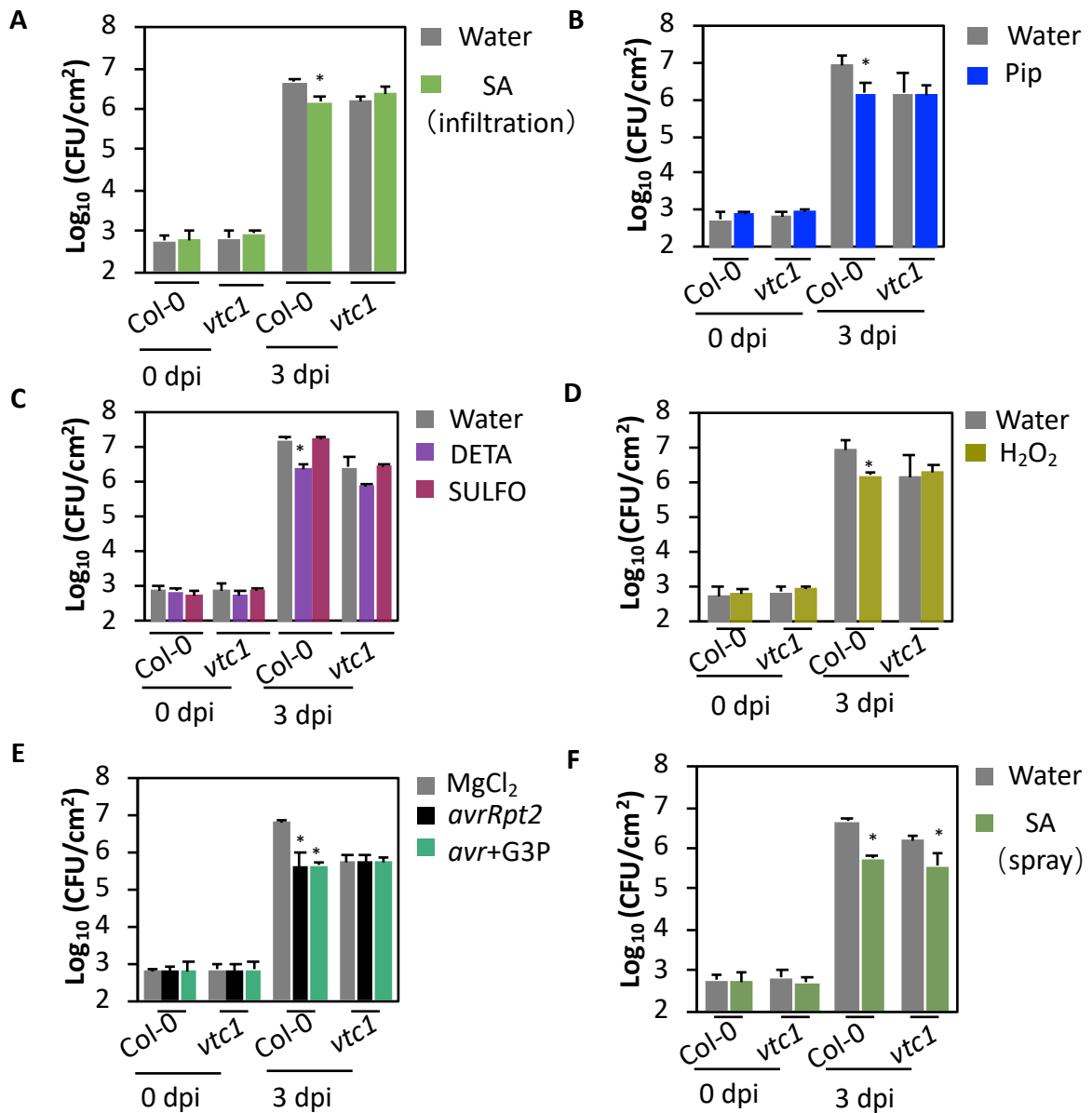
Fig. 5.4 Exogenous application of SA on whole plants increase the resistance of *vtc1*

(A-E) SAR response in distal leaves of WT Col-0 and *vtc1* plants treated locally with mock (MgCl$_2$ solution or water), SA (500 μM, A), Pip (1000 μM, B), NO donor (DETA, 100 μM, C), NO$_2$ donor (SULFO, 100 μM, C), H$_2$O$_2$ (100 μM, D), avirulent pathogen (*avrRpt2*) or G3P (100 μM, E) plus *avrRpt2*. The virulent pathogen (DC3000) was inoculated 48 hours after local treatments. Error bars indicate SD (*n* = 4). Asterisks denote a significant difference with mock (*t* test, *P* < 0.05). The experiment was repeated twice in a similar manner. **(F)** Responses of the Col-0 and *vtc1* upon infection with virulent *Pst DC3000* after

whole plant treating with SA. The virulent pathogen (DC3000) was inoculated 48 hours after whole plants were sprayed with 500 μM SA. Error bars indicate SD ($n = 4$). Asterisks denote a significant difference with mock (t test, $P < 0.05$). The experiment was repeated twice in a similar manner.

5.2.2 Comparison of *vtc1*, *vtc1 sid2* and *vtc1 ald1* plants for SAR, PTI and ETI

It has been shown previously in this chapter that the *vtc1* mutant exhibits high levels of expression level of *PR-1* and *ALD1* genes, which suggests that AsA-deficiency stimulates SA and Pip biosynthesis. To address the AsA relation between SA and Pip, double mutants *vtc1 sid2* and *vtc1 ald1* were generated. The *vtc1* plants exhibited curling leaves and long petioles, and usually were slightly smaller size than the Col-0 plants (Fig. 5.5A). The *vtc1 ald1* plants showed similar morphology as the *vtc1* plants, but the *vtc1 sid2* plants displayed a flat leaf phenotype (Fig. 5.5A), indicating that SA accumulation might affect plant morphology.

Mutation in *SID2* or *ALD1* failed to restore SAR in *vtc1* plants (Fig. 5.5B). And the *vtc1 sid2* and *vtc1 ald1* plants exhibited increased susceptibility to both avirulent *Pst avrRpt2* and virulent *Pst* DC3000 compared with the *vtc1* plants (Fig. 5.5C & D).
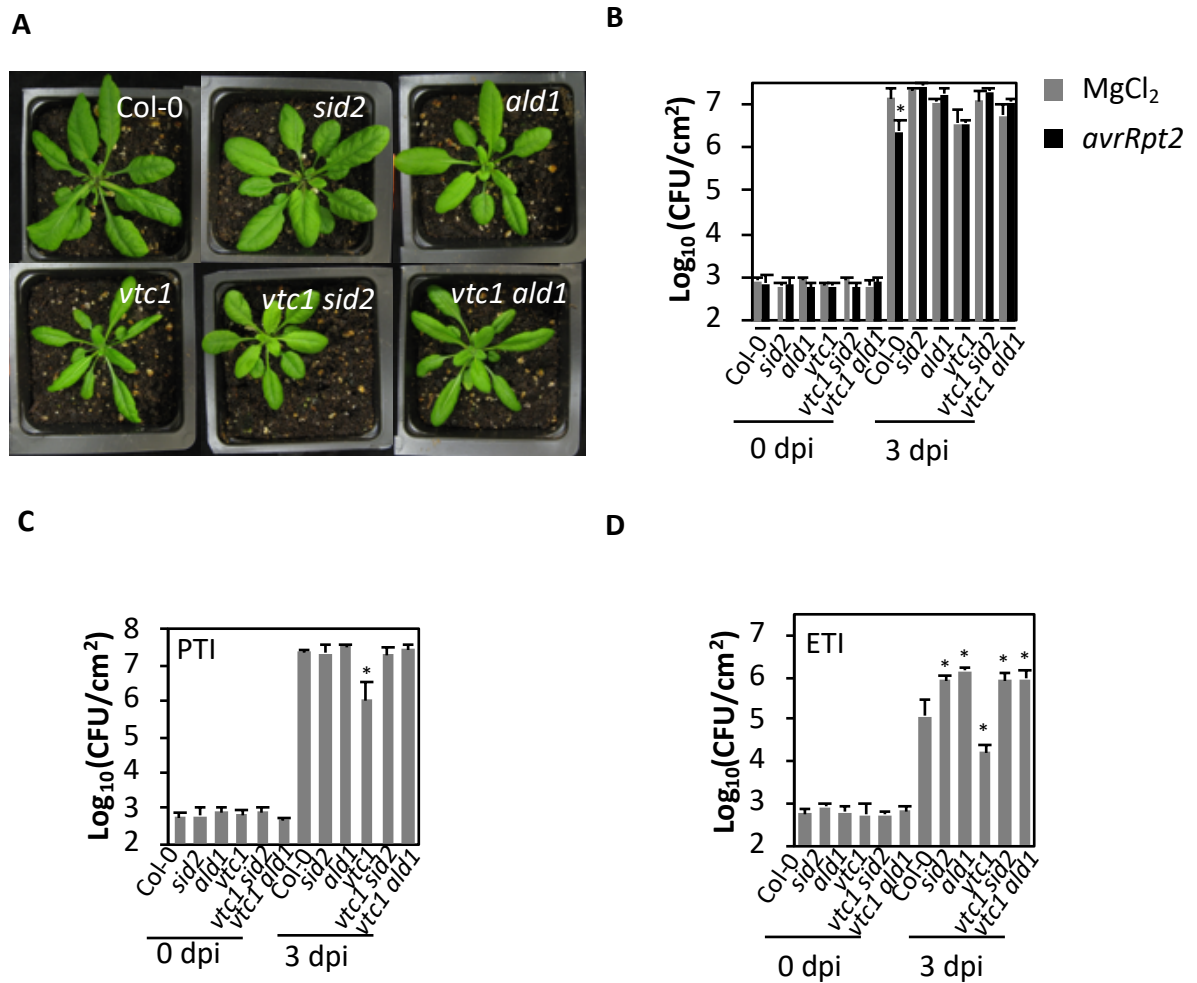
Fig. 5.5 Comparison of *vtc1*, *vtc1 sid2* and *vtc1 ald1* plants for SAR, PTI and ETI

(A) Morphology phenotypes of Col-0, *sid2*, *ald1*, *vtc1*, *vtc1 sid2*, *vtc1 ald1* plants. **(B)** SAR response in distal leaves of Col-0, *sid2*, *ald1*, *vtc1*, *vtc1 sid2*, *vtc1 ald1* plants treated locally with 10 mM $MgCl_2$ solution (mock) and avirulent pathogen (*avrRpt2*). The virulent pathogen (DC3000) was inoculated 48 hours after local treatments. Error bars indicate SD (n = 4). Asterisks denote a significant difference with mock (t test, $P < 0.05$). The experiment was repeated twice in a similar manner. **(C, D)** Responses of the Col-0, *sid2*, *ald1*, *vtc1*, *vtc1 sid2*, *vtc1 ald1* plants upon infection with virulent pathogen (*Pst* DC3000) (C) and avirulent pathogen (*Pst avrRpt2*) (D). The error bars represent SD (n = 4). Asterisks denote a significant difference with mock (t test, $P < 0.05$). The experiment was repeated twice with similar results.

5.2.3 Two different localized APX isoforms are required for SAR

In plants, APXs use AsA as a reducing compound to catalyze conversion of H_2O_2 into water, and thereby contribute to ROS level regulation. The Arabidopsis genome encodes eight APX isoforms, which are located in different subcellular compartments. A good understanding of the function of different localized APXs in SAR helps to trace ROS homeostasis in subcellular compartments during SAR. For this purpose, I first characterized the SAR phenotype of genetic mutants of three APX isoforms: APX1, s-APX and t-APX which are localized in the cytosol, chloroplast stroma and thylakoids, respectively. Salk_088596, Salk_083737 and Salk_027804 are the T-DNA insertion lines for *apx1*, *s-apx* and *t-apx* mutants, respectively. SAR assays showed that Salk_088596 and Salk_083737 but not Salk_027804 plants were compromised in *Pst avrRpt2*-mediated SAR (Fig. 5.6A), indicating that APX1 and S-APX are required for SAR. Because T-DNA insertion mutant has possibility of containing more than one insertion sites, to reconfirm the loss of SAR in Salk_088596 or Salk_083737 line is due to its mutation in *APX1* or *S-APX* gene, I selected another T-DNA line for each gene, Salk_000249 line for *APX1* and CS325715 line for *S-APX*. I tested SAR on Salk_000249 and CS325715 lines, and they were compromised in SAR (Fig. 5.6B). These results suggested that mutation in APX1 or S-APX impairs SAR. All the T-DNA insertion lines used in this study are genotyped as homozygous before use, and Salk_088596 and Salk_083737 lines were referred to as *apx1* and *s-apx*, respectively, in the following experiments.
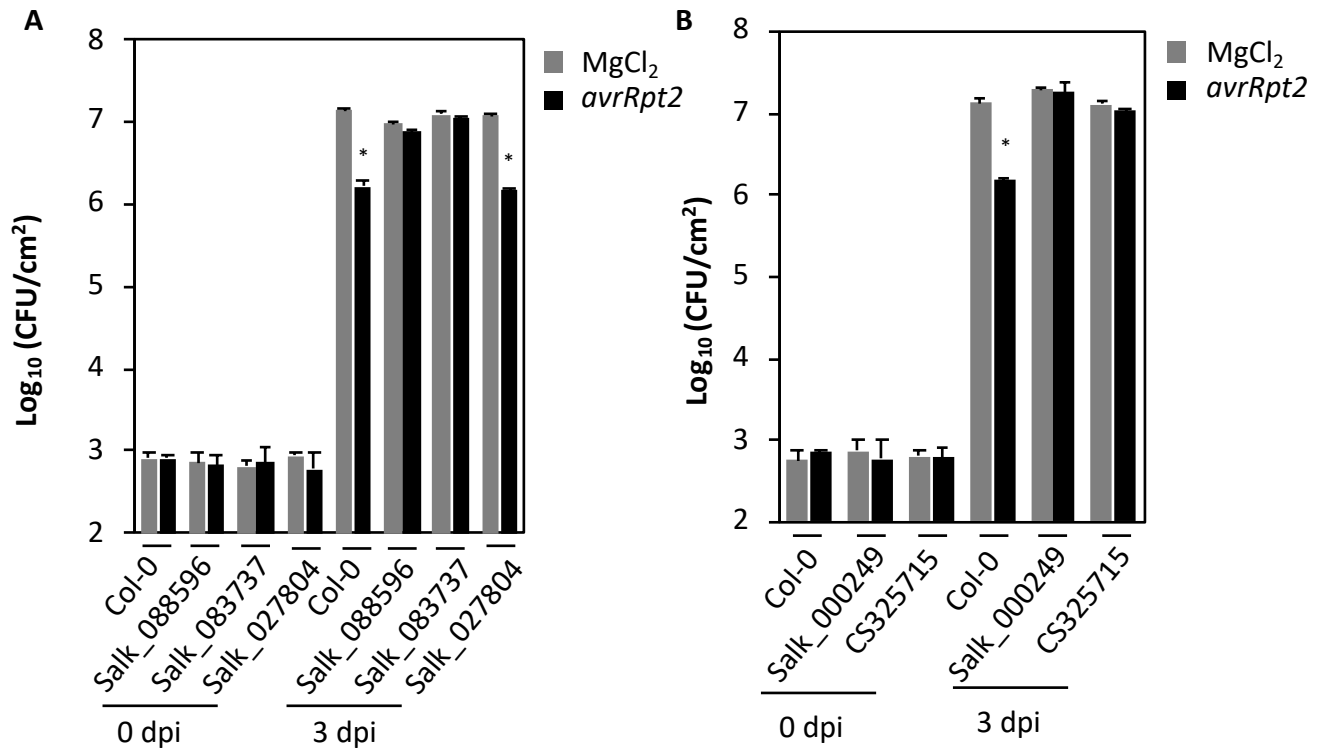
Fig. 5.6 *apx1* and *s-apx* are compromised in SAR

(A) SAR response in distal leaves of Col-0, Salk_088596, Salk_083737 and Salk_027804 plants treated locally with 10 mM $MgCl_2$ solution (mock) or avirulent pathogen (*avrRpt2*). The virulent pathogen (DC3000) was inoculated 48 hours after local treatments. Error bars indicate SD ($n = 4$). Asterisks denote a significant difference with mock (*t* test, $P < 0.05$). The experiment was repeated three in a similar manner. **(B)** SAR response in distal leaves of Col-0, Salk_000249 and CS325715 plants treated locally with 10 mM $MgCl_2$ solution (mock) or avirulent pathogen (*avrRpt2*). The virulent pathogen (DC3000) was inoculated 48 hours after local treatments. Error bars indicate SD ($n = 4$). Asterisks denote a significant difference with mock (*t* test, $P < 0.05$). The experiment was repeated twice in a similar manner.

5.2.4 Exogenous application of Pip restores SAR in *apx1* and *s-apx*

To understand the function of APX in the SAR pathway, I tested the effect of various SAR-associated chemicals in the *apx* mutant plants. Although localized application of SA failed to restore SAR in both *apx1* and *s-apx* (Fig. 5.7A), foliar spraying and root irrigating SA on the whole plants increased their resistance to the virulent pathogen (Fig. 5.7B), indicating that loss of APX1 or s-APX function affects the SA signaling transduction but does not affect these two mutants to perceive SA signal perception. Pip-NO/ROS-AzA-G3P is the other branch of the SAR signaling pathway. To understand whether the impaired SAR in *apx1* and *s-apx* is associated with the Pip-NO/ROS-AzA-G3P pathway, I assayed SAR with localized application of Pip, ROS, AzA or G3P. Neither of ROS, AzA or G3P was able to restore SAR on *apx1* or *s-apx* (Fig. 5.7C-E), but Pip (1000 μM) was able to restore SAR on these two mutants (Fig. 5.7F). GC-MS assay to quantify Pip levels in *apx1* and *s-apx*, and Pip accumulated in local tissues of these two mutants after avirulent pathogen *Pst avrRpt2* infection (Fig. 5.8), indicating that Pip is able to induce SAR in *apx1*, and that *s-apx* is not related to Pip biosynthesis.
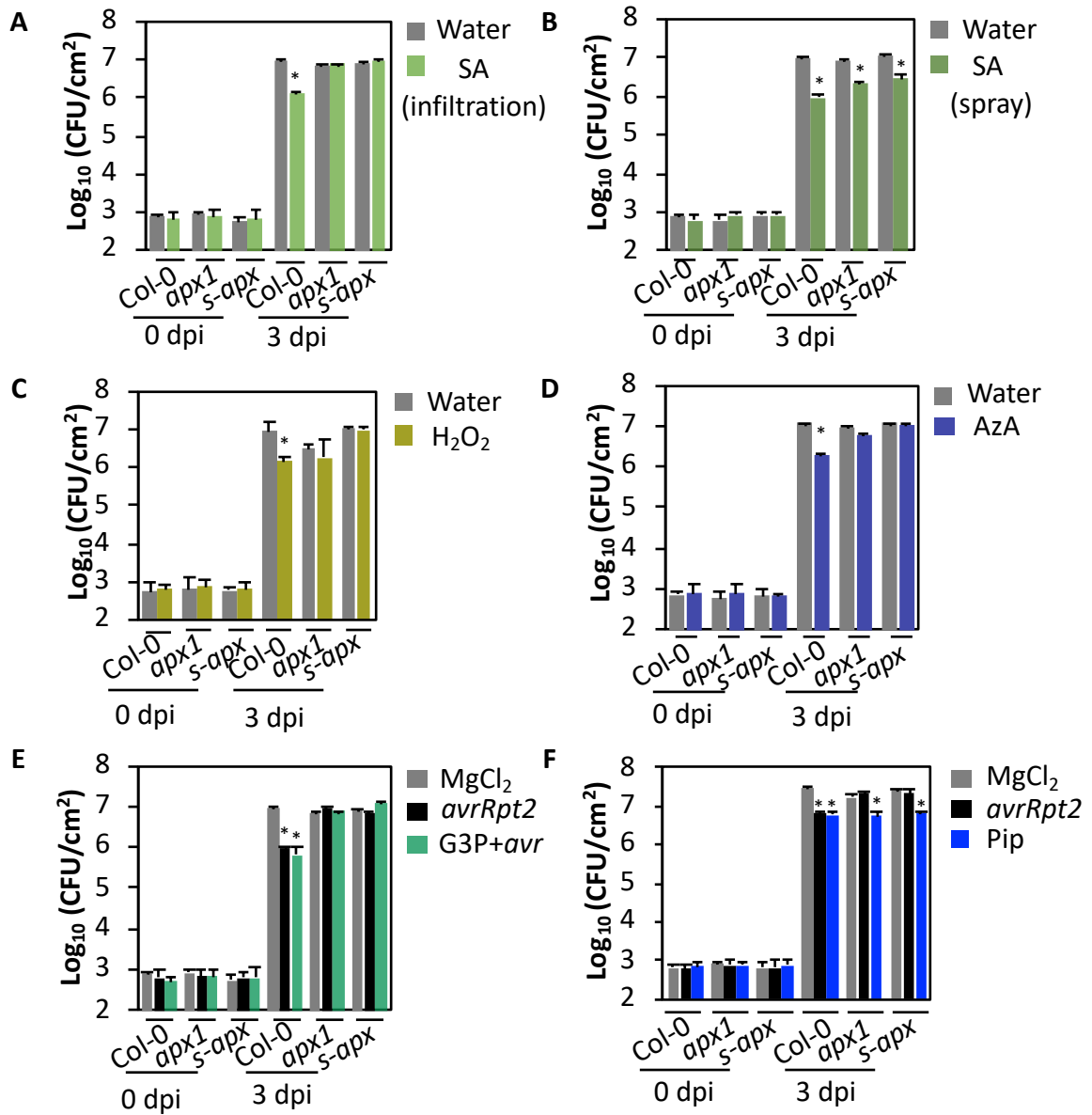
Fig. 5.7 SAR response with exogenous chemical application in *apx1* and *s-apx* plants

(A) SAR response in distal leaves of Col-0, *apx1* and *s-apx* plants treated locally with water (mock) and SA (500 μM). The virulent pathogen (*Pst* DC3000) was inoculated 48 hours after local treatments. Error bars indicate SD (*n* = 4). Asterisks denote a significant difference with mock (*t* test, $P < 0.05$). The experiment was repeated twice in a similar manner. **(B)** Responses of the Col-0, *apx1* and *s-apx* upon infection with *Pst DC3000* after whole plant treating with water (mock) and SA (500 μM). *Pst* DC3000 was inoculated 48

hours after whole plants were sprayed with 500 μM SA. Error bars indicate SD ($n = 4$). Asterisks denote a significant difference with mock (t test, $P < 0.05$). The experiment was repeated twice in a similar manner. **(C-F)** SAR response in distal leaves of WT Col-0, *apx1* and *s-apx* plants treated locally with mock (10 mM MgCl$_2$ solution or water), H$_2$O$_2$ (100 μM, C), AzA (100 μM, D), G3P (100 μM, E) plus *avrRpt2* or Pip (1000 μM, F). The virulent pathogen (*Pst* DC3000) was inoculated 48 hours after local treatments. Error bars indicate SD ($n = 4$). Asterisks denote a significant difference with mock (t test, $P < 0.05$). The experiment was repeated twice in a similar manner.
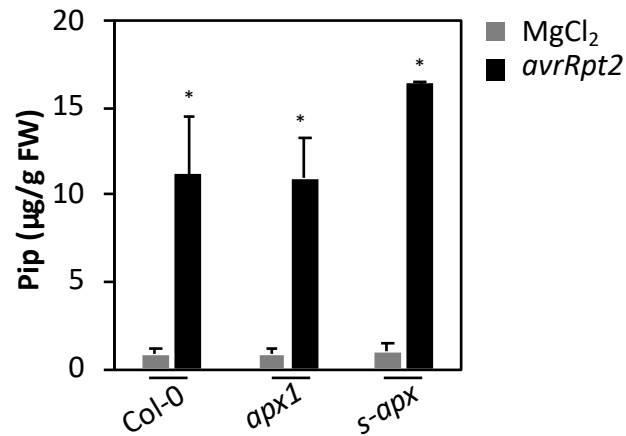
Fig. 5.8 Pip level in *apx1* and *s-apx* upon pathogen infection

Pip levels in local tissues of Col-0, *apx1* and *s-apx* plants after mock (10 mM MgCl$_2$ solution) and avirulent pathogen (*Pst avrRpt2*) inoculations. The leaves were sampled 48 hours after treatments. The error bars represent SD ($n = 4$). Asterisks denote a significant difference with mock (t test, $P < 0.05$). The experiment was repeated twice with similar results

5.3 Discussion

In this chapter, I characterized the SAR phenotype of mutants related to ascorbic acid biosynthesis and ascorbate peroxide. The results suggest that VTC1, VTC2, APX1 and S-APX are required for SAR. Both two AsA-deficient mutants *vtc1* and *vtc2* are compromised in SAR suggests that the inability of SAR in both mutants might be due to AsA deficiency but not the accumulation of their enzymic substrate or loss of their enzymic product for that VTC1 and VTC2 function in different steps of AsA biosynthesis. Interestingly, *vtc1* mutant accumulates high level SA and Pip which results in enhanced resistance of *vtc1* to both avirulent pathogen and virulent pathogen. This finding is also bridging connection between AsA and plant immune inducers SA and Pip. The deficiency of AsA results in the loss control of ROS level upon biotic and abiotic stress. However, when grown under optimal conditions, ROS level in *vtc1* plants shows no significant difference compared with WT plants (Veljovic-Jovanovic *et al*., 2001). However, in Chapter3, I showed that Pip is upstream ROS in SAR signaling and exogenous Pip induce ROS accumulation in wild-type plants. It is worthwhile to reconfirm the ROS level of *vtc1* plants. Further study in comparing the level of AsA, ROS, Pip and SA level in Col-0, *sid2*, *ald1*, *vtc1*, *vtc1 sid2* and *vtc1 ald1* plants will unveil the mystery between AsA and ROS, Pip or SA.

The finding that Pip confers SAR on both *apx1* and *s-apx* mutant will broaden our view about the model of SAR signaling pathway. APX1 and s-APX control ROS level in different subcellular compartment and the mutant lacking the function of APX1 or s-APX might affect their compartmental ROS homeostatic. Although in an entire plant cell level,

Pip is able to induce ROS and downstream signaling, consequently inducing SAR, but in

subcellular level, the interaction between Pip-ROS will need further study.

APPENDIX-A

LIST OF ABBREVIATIONS

Acronym/ abbreviation	Expansion
L/mL/µL	Liter/milliliter/microliter
M/mM/µM	Molar/millimolar/micromolar
g/mg/µg/ng	Gram/milligram/microgram/nanogram
h/min/sec	Hours/minutes/seconds
RH	Relative humidity
°C	Centigrade degree
18:0	Stearic acid
18:1	Oleic acid
18:2	Linoleic acid
18:3	Linolenic acid
AA	Acetic acid
AsA	L-ascorbic acid
AzA	Azelaic acid
BSA	Bovine serum albumin
BHT	Butylated hydroxytoluene
BTH	Benzo [1,2,3] thiadiazole-7-carbothioic Acid *S*-Methyl Ester
CaCl$_2$	Calcium chloride
CAPS	Cleaved amplified polymorphic sequences
dATP	Deoxyribo adenosine triphosphate
dCAPS	Derived cleaved amplified polymorphic sequences
dCTP	Deoxyribo cytosine triphosphate
DEPC	Diethyl pyrocarbonate
DMSO	Dimethyl sulfoxide
DNA	Deoxyribonucleic acid
dGTP	Deoxyribo guanidine triphosphate
DHAP	Dihydroxyacetone phosphate
dNTP	Deoxyribo nucleic triphosphate
dpi	Day post inoculation
DTT	Dithiothreitol
DGDG	Digalactosyldiacylglycerol
EDTA	Ethylene diamine tetra acetic acid
EtBr	Ethidium bromide
FA	Fatty acid
FW	Fresh weight

G3P	Glycerol-3-phosphate
GC-MS	Gas chromatography-mass spectrometry
HCl	Hydrochloric acid
IPTG	Isopropyl β-D-1-thiogalactopyranoside
K_2HPO_4	Potassium phosphate, dibasic
KH_2PO_4	Potassium phosphate, monobasic
KCl	Potassium chloride
KOH	Potassium hydroxide
LB	Luria-Bertani
MGDG	Monogalactosyldiacylglycerol
MeSA	Methyl salicylic acid
$MgCl_2$	Magnesium chloride
$MgSO_4$	Magnesium sulfate
MOPS	3-(N-morpholino) propanesulfonic acid
MS	Murashige and Skoog
NaCl	Sodium chloride
NaAc	Sodium acetate
NaOH	Sodium hydroxide
Na_2HPO_4	Sodium hydrogen phosphate
$NaPO_4$	Sodium phosphate
NHP	N-hydroxypipecolic acid
N-OGlc-Pip	N-hydroxypipecolic glucoside
NPT	Neomycin phosphor transferase
PCR	Polymerase chain reaction
PBS	Phosphate-buffered saline
Pip	Pipecolic acid
R	Resistant or resistance
RNA	Ribonucleic acid
SA	Salicylic acid
SAG	Salicylic acid glucoside
SD	Standard deviation
SDS	Sodium dodecyl sulfate
SE	Standard error
SSC	Sodium chloride, sodium citrate
TBE	Tris-borate/EDTA electrophoresis buffer
TE	Tris-EDTA
WT	Wild type

APPENDIX-B

LIST OF ABBREVIATIONS OF GENES USED IN THIS STUDY

Acronym/ abbreviation	Expansion
ALD1	AGD2-LIKE DEFENSE PROTEIN 1
APX1	ASCORBATE PEROXIDASE
AZI1	AZELAIC ACID INDUCED 1
DGD1	DIGALACTOSYL DIACYLGLYCEROL SYNTHASE 1
DIR1	DEFECTIVE IN INDUCED RESISTANCE 1
EDS1	ENHANCED DISEASE SUSCEPTIBILITY 1
EDS5	ENHANCED DISEASE SUSCEPTIBILITY 5
FMO1	FLAVIN-CONTAININGG MONOOXYGENASE
ICS1	ISOCHORISMATE SYNTHASE1
MGD1	MONOGALACTOSYL DIACYLGLYCEROL SYNTHASE 1
NOA1	NITRIC OXIDE ASSOCIATED 1
NPR1	NONEXPRESSER OF PR GENES 1
PAD4	PHYTOALEXIN DEFICIENT 4
RBOHD	RESPIRATORY BURST OXIDASE PROTEIN D
RBOHF	RESPIRATORY BURST OXIDASE PROTEIN F
s-APX	s-ASCORBATE PEROXIDASE
SARD4	SAR DEFICIENT 4
SID2	SALICYLIC ACID INDUCTION DEFICIENT 2
SOX	SARCOSINE OXIDASE
t-APX	t-ASCORBATE PEROXIDASE
VTC1	VITAMIN C DEFECTIVE 1
VTC2	VITAMIN C DEFECTIVE 2
VTC3	VITAMIN C DEFECTIVE 3
VTC4	VITAMIN C DEFECTIVE 4
VTC5	VITAMIN C DEFECTIVE 5

REFERENCES

Agius F, González-Lamothe R, Caballero JL, Muñoz-Blanco J, Botella MA, Valpuesta V. (2003) Engineering increased vitamin C levels in plants by overexpression of a D-galacturoninc acid reductase. *Nat. Biothechnol.* 21: 177-181.

Barth C, Moeder W, Klessig DF, Conklin PL. (2004) The timing of senescence and response to pathogens is altered in the ascorbate-deficient Arabidopsis mutant *vitamin c-1*. *Plant Physiol.* 134(4): 1784-1792.

Bartsch M, Gobbato E, Bednarek P, Debey S, Schultze JL, Bautor J, Parker JE. (2006) Salicylic acid-independent EHANCED DISEASE SUSCEPTIBILITY 1 singaling in *Arabidopsis* immunity and cell death is regulated by the monooxygenase *FMO1* and the nudix hydrolase *NUDT7*. *Plant Cell* 18(4): 1038-1051.

Bernsdorff F, Döring A-C, Gruner K, Schuck S, Bräutigam A, Zeier J. (2016) Pipecolic acid orchestrates plant systemic acquired resistance and defense priming via salicylic acid-dependent and -independent pathways. *Plant Cell* 28(1): 102-129.

Broquist HP. (1991) Lysine-pipecolic acid metabolic relationships in microbes and mammals. *Annu. Rev. Nutr.* 11: 435-448.

Bürger M, Chory J. (2019) Stressed out about hormones: how plants orchestrate immunity. *Cell Host Microbe* 26(2): 163-172.

Chamizo-Ampudis A, Sanz-Luque E, Llamas A, Galvan A, Fernandez EJ. (2017) Nitrate reductase regulates plant nitric oxide homeostasis. *Trends Plant Sci.* 22: 163-174.

Cao H, Glazebrook J, Clarke JD, Volko S, Dong X. (1997) The Arabidopsis NPR1 gene that controls systemic acquired resistance encodes a novel protein containing ankyrin repeats. *Cell* 88(1): 57-63.

Cao X, Yang H, Shang C, Ma S, Liu L, Cheng J. (2019) The roles of auxin biosynthesis YUCCA gene family in plants. *Int. J. Mol. Sci.* 20(24): 6343.

Caverzan A, Passaia G, Rosa SB, Ribeiro CW, Lazzarotto F, Margis-Pinheiro M. (2012) Plant responses to stresses: Role of ascorbate peroxidase in the antioxidant protein. *Genet. Mol. Bio.* 35(4 Suppl.): 1011-1019.

Cecchini NM, Jung HW, Engle NL, Tschaplinski TJ, Greenberg JT. (2015) AlD1 regulates basal immune components and early inducible defense responses in *Arabidopsis*. Mol. *Plant Microbe Interact.* 28(4): 455-466.

Chanda B, Venugopal SC, Kulshrestha S, Navarre DA, Downie B, Vaillancourt L, Kachroo A, Kachroo P. (2008) Glycerol-3-phosphate levels are associated with basal resistance to the hemibiotrophic fungus Colletotrichum higginsianum in Arabidopsis. *Plant Physiol.* 147(4): 2017-2029.

Chanda B, Xia Y, Mandal MK, Yu K, Sekine KT, Gao QM, Selote D, Hu Y, Stromberg A, Navarre D, Kachroo A, Kachroo P. (2011) Glycerol-3-phosphate is a critical mobile inducer of systemic immunity in plants. *Nat. Genet.* 43(5): 421-427.

Chandra-Shekara AC, Navarre D, Kachroo A, Kang H-G, Klessig D, Kachroo P. (2004) Signaling requirements and role of salicylic acid in HRT- and rrt- mediated resistance to turnip crinkle virus in Arabidopsis. *Plant J.* 40: 647-659.

Chandra-Shekara AC, Gupte M, Navarre D, Raina S, Raina R, Klessig D, Kachroo P. (2006) Light-dependent hypersensitive response and resistance signaling against *Turnip Crinkle Virus* in *Arabidopsis*. *Plant J.* 45(3): 320-334.

Chen YC, Holmes EC, Rajniak J, Kim JG, Tang S, Fischer CR, Mudgett MB, Sattely ES. (2018) N-hydroxy-pipecolic acid is a mobile metabolite that induces systemic disease resistance in Arabidopsis. *Proc. Natl. Acad. Sci. U. S. A.* 115(21): E4920-E4929.

Chester KS. (1933) The problem of acquired physiological immunity in plants. *Q. Rev. Biol.* 8: 275-324.

Clarke JD, Aarts N, Feys BJ, Dong X, Parker JE. (2001) Constitutive disease resistance requires EDS1 in the Arabidopsis mutants cpr1 and cpr6 and is partially EDS1-dependent in cpr5. *Plant J.* 26(4): 409-420.

Clough SJ, Bent AF. (1998) Floral dip: a simplified method for Agrobacterium- mediated transformation of Arabidopsis thaliana. *Plant J.* 16(6):735-743.

Crawford NM. (2006) Mechanisms for nitric oxide synthesis in plants. *J. Exp. Bot.* 57(3): 471-478.

Cui F, Wu S, Sun W, Coaker G, Kunkel B, He P, Shan L. (2013) The Pseudomonas syringae type III effector AvrRpt2 promotes pathogen virulence via stimulating Arabidopsis auxin/indole acetic acid protein turnover. *Plant Physiol.* 162: 1018-1029.

Conklin PL, Gatzek S, Wheeler GL, Dowdle J, Raymond MJ, Rolinski S, Isupov M, Littlechild JA, Smirnoff N. (2006) *Arabidopsis thaliana VTC4* encodes L-galactose-1-P phosphatase, a plant ascorbic acid biosynthetic enzyme. *J. Biol. Chem.* 281(23): 15662-15670.

Conklin PL, Norris SR, Wheeler GL, Williams EH, Smirnoff N, Last RL. (1999) Genetic evidence for the role of GDP-mannose in plant ascorbic acid (vitamin C) biosynthesis. *Proc. Natl. Acad. Sci. U. S. A.* 96(7): 4198-4203.

Conklin PL, Saracco SA, Norris SR, Last RL. (2000) Identification of ascorbic acid-deficient *Arabidopsis thaliana* mutants. *Genetics.* 154(2): 847-856.

Conklin PL, Williams EH, Last RL. (1996) Environmental stress sensitivity of an ascorbic acid-deficient Arabidopsis mutant. *Proc. Natl. Acad. Sci. U. S. A.* 93(18): 9970-9974.

Dangl JL, Dietrich RA, Richberg MH. (1996) Death don't have no mercy: cell death programs in plant-microbe interactions. *Plant Cell* 8(10): 1793-1807.

Dangl JL, Horvath DM, Staskawicz BJ. (2013) Pivoting the plant immune system from dissection to deployment. *Science* 341: 746-751.

Daudi A, O'Brien JA. (2012) Detection of hydrogen peroxide by DAB staining in *Arabidopsis* leaves. *Bio-Protoc*. 2: e263.

Dempsey DA, Vlot AC, Wildermuth MC, Klessig DF. (2011) Salicylic acid biosynthesis and metabolism. *Arabidopsis Book* 9: e0156.

Ding P, Rekhter D, Ding Y, Feussner K, Busta L, Haroth S, Xu S, Li X, Jetter R, Feussner I, Zhang Y. (2016) Characterization of a pipecolic acid biosynthesis pathway required for systemic acquired resistance. *Plant Cell* 28(10): 2603-2615.

Dixon RA. (1986) The phytoalexin response: elicitation, signaling, and control of host gene expression. *Biol. Rev. Camb. Philos. Soc.* 61: 239-292.

Durrant WE, Dong X. Systemic acquired resistance. (2004) *Annu. Rev. Phytopathol.* 42: 185-209.

Fischer RA, Byerlee D, Edmeades GO. (2014) Crop yields and global food security: will yield increase continue to feed the world? *ACIAR Monograph* No. 158. Australian Centre for International Agricultural Research.

Flor H. (1971) Current status of gene-for-gene concept. *Annu. Rev. Phytopathol.* 9: 275-296.

Gao QM, Yu K, Xia Y, Shine MB, Wang C, Navarre D, Kachroo A, Kachroo P. (2014) Mono- and digalactosyldiacylglycerol lipids function nonredundantly to regulate systemic acquired resistance in plants. *Cell Rep.* 9(5): 1681-1691.

Gaupels F, Durner J, Kogel KH. (2017) Production, amplification and systemic propagation of redox messengers in plants? The phloem can do it all! *New Phytol.* 214(2): 554-560.

Goyer A, Johnson TL, Olsen LJ, Collakova E, Schachar-Hill Y, Rhodes D, Hanson AD. (2004) Characterization and metabolic function of a peroxisomal sacosine and pipecolate oxidase from Arabidopsis. *J. Biol. Chem.* 279(17): 16947-16953.

Gill US, Lee S, Mysore KS. (2015) Host versus nonhost resistance: distinct wars with similar arsenals. *Phytopathology* 105(5): 580-587.

Hartmann M, Kim D, Bernsdorff F, Ajami-Rashidi Z, Scholten N, Schreiber S, Zeier T, Schuck S, Reichel-Deland V, Zeier J. (2017) Biochemical principles and functional aspects of pipecolic acid biosynthesis in plant immunity. *Plant Physiol.* 174(1): 124-153.

Hartmann M, Zeier T, Bernsdorff, Reichel-Deland V, Kim D, Hohmann M, Scholten N, Schuch S, Bräutigam A, Hölzel T, Ganter C, Zeier J. (2018) Flavin monooxygenase-generated N-hydroxypipecolic acid is a critical element of plant systemic immunity. *Cell* 173(2): 456-469.

Hansen BG, Kliebenstein DJ, Halkier BA. (2007) Identification of a flavin-monooxygenase as the S-oxygenating enzyme in aliphatic glucosinolate biosynthesis in Arabidopsis. *Plant J.* 50: 902-910.

Li J, Hansen BG, Ober JA, Kliebenstein DJ, Halkier BA. (2008) Subclade of Flavin-Monooxygenases involved in aliphatic glucosinolate biosyntheis. *Plant Physiol.* 148(3): 1721-1733.

Lindermayr C, Sell S, Müller B, Leister D, Durner J. (2010) Redox regulation of the NPR1-TGA1 system of Arabidopsis thaliana by nitric oxide. *Plant Cell* 22(8): 2894-2907.

Linster CL, Clarke SG. (2008) L-Ascorbate biosynthesis in higher plants: the role of VTC2. *Trends Plant Sci.* 13(11): 576-573.

Linster CL, Gomez TA, Christensen KC, Adler LN, Young BD, Brenner C, Clarke SG. (2007) Arabidopsis *VTC2* encodes a GDP-L-galactose phosphorylase, the last unknown enzyme in the Smirnoff-Wheeler pathway to ascorbic acid in plants. *J. Biol. Chem.* 282(26):18879-18885.

Lipka U, Fuchs R, Lipka V. (2008) Arabidopsis non-host resistance to powdery mildews. *Curr. Opin. Plant Biol.* 11(4): 404-411.

Jirage D, Tootle TL, Reuber TL, Frost LN, Feys BJ, Parker JE, Ausubel FM, Glazebrook J. (1999) Arabidopsis thaliana PAD4 encodes a lipase-like gene that

is important for salicylic acid signaling. *Proc. Nati. Acad. Sci. U. S. A.* 96(23): 13583-13588.

Jones JDG, Dangl JL. (2006) The plant immune system. *Nature* 444: 323-329.

Jung HW, Tschaplinski TJ, Wang L, Glazebrook J, Greenberg JT. (2009) Priming in systemic plant immunity. *Science* 324: 89-91.

Kachroo A, Lapchyk L, Fukushigae H, Hildebrand D, Klessig D, Kachroo P. (2003) Plastidial fatty acid signaling modulates salicylic acid- and jasmonic acid- mediated defense pathways in Arabidopsis *ssi2* mutant. *Plant Cell* 12: 2952-2965.

Kachroo A, Kachroo P. (2007) Salicylic acid-, jasmonic acid- and ethylene-mediated regulation of plant defense signaling. In: Setlow JK (eds) Genetic Engineering. *Genetic Engineering* 28: 55-83.

Kachroo P, Chandra-Shekara AC, Klessig DF. (2006) Plant signal transduction and defense against viral pathogens. *Adv. Virus Res.* 66: 161-191.

Kauss H. (1987) Some aspects of calcium-dependent regulation in plant metabolism. *Annu. Rev. Plant Physiol.* 38: 47-72.

Koch E, Slusarenko A. (1990) Arabidopsis is susceptible to infection by a downy mildew fungus. *Plant Cell* 2(5): 437-445.

Koch M, Vorwerk S, Masur C, Sharifi-Sirchi G, Olivieri N, Schlaich NL. (2006) A role of a flavin-containing mono-oxygenase in resistance against microbial pathogens in Arabidopsis. *Plant J.* 47(4): 629-639.

Lim GH, Shine MB, de Lorenzo L, Yu K, Cui W, Navarre D, Hunt AG, Lee JY, Kachroo, Kachroo P. (2016) Plasmodesmata localizing proteins regulate transport

and signaling during systemic acquired immunity in plants. *Cell Host Microbe* 19(4): 541-549.

Lorence A, Chevone BI, Mendes P, Nessler CL. (2004) *myo*-inositol oxygenase offers a possible entry point into plant ascorbate biosynthesis. *Plant Physiol.* 134(3): 1200-1205.

Low PS, Merida JR. (1996) The oxidative burst in plant defense: Function and signal transduction. *Physiol. Plant* 96: 533-542.

Mandal MK, Chanda B, Xia Y, Yu K, Sekine K, Gao QM, Selote D, Kachroo A, Kachroo P. (2011) Glycerol-3-phosphate and systemic immunity. *Plant Signal Behav.* 6(11): 1871-1874.

Mandal MK, Chandra-Shekara AC, Jeong RD, Yu K, Zhu S, Chanda B, Navarre D, Kachroo A, Kachroo P. (2012) Oleic acid-dependent modulation of NITRIC OXIDE ASSOCIATED 1 protein levels regulates nitric oxide-mediated defense signaling in Arabidopsis. *Plant Cell* 24(4): 1654-1674.

Maldonado AM, Doerner P, Dixon RA, Lamb CJ, Cameron RK. (2002) A putative lipid transfer protein involved in systemic resistance signaling in Arabidopsis. *Nature* 419: 399-403.

Martin K, Kopperud K, Chakrabarty R, Banerjee R, Brooks R, Goodin MM. (2009) Transient expression in Nicotiana benthamiana fluorescent marker lines provides enhanced definition of protein localization, movement and interactions *in planta*. *Plant J.* 59: 150-162.

McDonald BA, Stukenbrock EH. (2016) Rapid emergence of pathogens in agro-ecosystems: global threats to agricultural sustainability and food security. *Phil.Trans. R. Soc. B* 371: 20160026.

Melotto M, Underwood W, Koczan J, Nomura K, He SY. (2006) Plant stomata function in innate immunity against bacterial invasion. *Cell* 126: 969–980.

Melotto M, Zhang L, Oblessuc PR, He SY. (2017) Stomatal defense a decade later. *Plant Physiol.* 174: 561–571.

Mishina TE, Zeier J. (2006) The Arabidopsis flavin-dependent monooxygenase FMO1 is an essential component of biologically induced systemic acquired resistance. *Plant Physiol.* 141(4): 1666-1675.

Nakagawa T, Suzuki T, Murata S, Nakamura S, Hino T, Maeo K, Tabata R, Kawai T, Tanaka K, Niwa Y, Watanabe Y, Nakamura K, Kimura T, Ishiguro S. (2007) Improved Gateway binary vectors: high-performance vectors for creation of fusion constructs in transgenic analysis of plants. *Biosci. Biotechnol. Biochem.* 71(8): 2095-2100.

Návarová H, Bernsdorff F, Doring AC, Zeier J. (2012) Pipecolic acid, an endogenous mediator of defense amplification and priming, is critical regulator of inducible plant immunity. *Plant Cell* 24: 5123-5141.

Nishiya Y, Abe Y. (2015) Comparison of the substrate specificity of L-pipecolate oxidase and bacterial monomeric sarcosine oxidase, and structural interpretation of the enzymes. *Int. J. Anal. Bio-Sci.* 3(3): 55-62.

Oerke EC. (2006) Crop losses to pests. *J. Agric. Sci.*144, 31-43.

Olszak B, Malinovsky FG, Brodersen P, Grell M, Giese H, Petersen M, Mundy J. (2006) A putative flavin-containing monooxygenase as a marker for certain defense and cell death pathways. *Plant Sci.* 170(3): 614-623.

Park SW, Kaimoyo E, Kumar D, Mosher S, Klessig DF. (2007) Mehtyl salicylate is a critical mobile signal for plant systemic acquired resistance. *Science* 318:113-116.

Pieterse CMJ, Leon-Reyes A, Van der Ent S, Van Wees SCM. (2009) Networking by small-molecules hormones in plant immunity. *Nat. Chem. Biol.* 5: 308-316.

Pieterse CMJ, Van der Does D, Zamioudis C, Leon-Reys A, Van Wees SCM. (2012) Hormonal modulation of plant immunity. *Annu. Rev. Cell Dev. Biol.* 28: 489-521.

Poulsen LL, Ziegler DM. (1995) Multisubstrate flavin-containing monooxygenases: applications of mechanism to specificity. *Chem. Biol. Interact.* 96(1): 57-73.

Rekhter D, Lüdke D, Ding Y, Feussner K, Zienkiewicz K, Lipka V, Wiermer M, Zhang Y, Feussner I. (2019a) Isochorismate-derived biosynthesis of the plant stress hormone salicylic acid. *Science* 365(6452): 498-502.

Rekhter D, Mohnike L, Feussner K, Zienkiewicz K, Zhang Y, Feussner I. (2019b) Enhanced disease susceptibility 5 (EDS5) is required for N-hydroxy pipecolic acid formation. bioRxiv doi: https://doi.org/10.1101/630723.

Ross AF. (1961) Systemic acquired resistance induced by localized virus infections in plants. *Virology* 14: 340-358.

Ryals J, Uknes S, Ward E. (1994) Systemic acquired resistance. *Plant Physiol.* 104: 1109-1112.

Schlaich NL. (2007) Flavin-containing monooxygenases in plants: looking beyong detox. Trends *Plant Sci.* 12(9): 412-418.

Schwessinger B, Ronald PC. (2012) Plant innate immunity: perception of conserved microbial signatures. *Annu. Rev. Plant Biol.* 63: 451-482.

Serrano M, Wang B, Aryal B, Garcion C, Abou-Mansour E, Hech S, Geisler M, Mauch F, Nawrath C, Métraux J-P. (2013) Export of salicylic acid from the chloroplast requires the multidrug and toxin extrusion-like transporter EDS5. *Plant Physiol.* 162: 1815-1821.

Shigeoka S, Ishikawa T, Tamoi M, Miyagawa Y, Takeda T, Yabuta Y, Yoshimura K. (2002) Regulation and function of ascorbate peroxidase isoenzymes. *J. Exp. Bot.* 53(372): 1305-1319.

Shine MB, Yang J-W, EI-Habbak M, Nagyabhyru P, Fu D-Q, Navarre D, Ghabrial S, Kachroo P, Kachroo A. (2016) Cooperative functioning between phenylalanine ammonia lyase and isochorismate synthase activities contributes to salicylic acid biosynthesis in soybean. *New Phytol.* 212(3): 627-636.

Shine MB, Xiao X, Kachroo, P, Kachroo A. (2018) Signaling mechanisms underlying systemic acquired resistance of microbial pathogens. *Plant Sci.* 279: 81-86.

Sobolev V, Edelman M, Dym O, Unger T, Albeck S, Kirma M, Galili G. (2013) Structure of ALD1, a plant-specific homologue of the unversal diaminopimelate aminotransferase enzyme of lysine biosyntheis. *Acta. Crystallogr. Sect. F Struct. Biol. Cryst. Commun.* 69(Pt 2): 84-89.

Tada T., Spoel SH, Pajerowska-Mukhtar K, Mou Z, Song J, Wang C, Zuo J, Dong X. (2008) Plant immunity requires conformational changes of NPR1 via S-nitrosylation and thioredoxins. *Science* 321(5891): 952-956.

Torrens-Spence MP, Bobokalonova A, Carballo V, Glinkerman CM, Pluskal T, Shen A, Weng J-K. (2019) PBS3 and EPS1 complete salicylic acid biosynthesis from isochorismate in Arabidopsis. *Mol. Plant* 12(12): 1577-1586.

Torres MA, Dangl JL, Jones JDG. (2002) *Arabidopsis* gp91^{phox} homologues *AtrbohD* and *AtrobhF* are required for accumulation of reactive oxygen intermediates in the plant defense response. *Proc. Natl. Acad. Sci. U. S. A.* 99(1): 517-522.

Uknes S, Mauch-Mani B, Moyer M, Potter S, Williams S, Dincher S, Chandler D, Slusarenko A, Ward E, Ryals J. (1992) Acquired resistance in Arabidopsis. *Plant Cell* 4: 645-656.

Vance CP, Kirk TK, Sherwood RT. (1980) Lignification as a mechanism of disease resistance. *Annu. Rev. Phytopathol.* 18: 259-288.

van de Wouw M, Kik C, van Hintum T, van Treuren R, Visser B. (2010) Genetic erosion in crops: concept, research results and challenges. *Plant Genet. Resour.* 8: 1-15.

Van Loon LC, Antoniw JF. (1982) Comparison of the effects of salicylic acid and ethephon with virus-induced hypersensitivity and acquired resistance in tobacco. *Neth. J. Plant Pathol.* 88: 237-256.

Veljovic-Jovanovic SD, Pignocchi C, Noctor G, Foyer CH. (2001) Low ascorbic acid in the *vtc-1* mutant of Arabidopsis is associated with decreased growth and intracellular redistribution of the antioxidant system. *Plant Physiol.* 127(2): 426-435.

Vlot AC, Dempsey DA, Klessig DF. (2009) Salicylic acid, a multifaceted hormone to combat disease. *Ann. Rev. Phytopath.* 47: 177-206.

Ward ER, Uknes SJ, Williams SC, Dincher SS, Wiederhold DL, Alexander DC, Ahl-Goy P, Métraux J-P, Ryals JA. (1991) Coordinate gene activity in response to agents that induce systemic acquired resistance. *Plant Cell* 3: 1085-1094.

Wang C, El-Shetehy M, Shine MB, Yu K, Navarre D, Wendehenne D, Kachroo A, Kachroo P. (2014) Free radicals mediate systemic acquired resistance. *Cell Rep.* 7(2): 348-355.

Wang C, Liu R, Lim GH, de Lorenzo L, Yu K, Zhang K, Hunt AG, Kachroo A, Kachroo P. (2018) Pipecolic acid confers systemic immunity by regulating free radical. *Sci. Adc.* 4(5): eaar4509.

Wendehenne D, Gao QM, Kachroo A, Kachroo P. (2014) Free radical-mediated systemic immunity in plants. *Curr. Opin. Plant Biol.* 20: 127-134.

Wheeler GL, Jones MA, Smirnoff N. (1998) The biosynthetic pathway of vitamin C in higher plants. *Nature* 393(6683): 365-369.

Wildermuth MC, Dewdney J, Wu G, Ausubel FM. (2001) Isochorismate synthase is required to synthesize salicylic acid for plant defense. *Nature* 414: 562-565.

Wilkinson JQ, Crawford NM. (1993) Identification and characterization of a chlorate-resistant mutant of *Arabidopsis thaliana* with mutations in both nitrate reductase structural genes *NIA1* and *NIA2*. *Mol. Gen. Genet.* 239: 289-297.

Withers J, Dong X. (2016) Posttrasnslational modifications of NPR1: a single protein playing multiple roles in plant immunity and physiology. *PLoS Pathog.* 12(8):e1005707.

Wolucka BA, Van Montagu M. (2003) GDP-mannose 3´,5´-epimerase forms GDP-L-gulose, a putative intermediate for the *de novo* biosynthesis of vitamin C in plants. *J. Biol. Chem.* 278(48): 47483-47490.

Xin XF, Kvitko B, He SY. (2018) *Pseudomonas syringae*: what is takes to a pathogen. *Nat. Rev.* 16:316-328.

Yu K, Soares JM, Mandal MK, Wang C, Chanda B, Gifford AN, Fowler JS, Navarre D, Kachroo A, Kachroo P. (2013) A feedback regulatory loop between G3P and lipid transfer proteins DIR1 and AZI1 mediates azelaic-acid-induced systemic immunity. *Cell Rep.* 3(4): 1266-1278.

Zhu S, Jeong RD, Venugopal SC, Lapchyk L, Navarre D, Kachroo A, Kachroo P. (2011) SAG101 forms a ternary complex with EDS1 and PAD4 and is required for resistance signaling against Turnip Crinkle Virus. *PLoS Pathog.* 7: e1002318.

Ziegler DM, Pettit FH. (1964) Formation of an intermediate N-oxide in the oxidative demethyiation of N,N´-dimethyianiline catalyzed by liver microbes. *Biochem. Biophys. Res. Commun.* 15(2): 188-193.

Ziegler DM. (2002) An overview of the mechanism, substrate specificities, and structure of FMOs. *Drug. Metab. Rev.* 34(3): 503-511.

Zipfel C. (2014) Plant pattern-recognition receptors. *Trends Immunol.* 35(7): 345-351.

RUIYING LIU

Education

M.S.	Plant Pathology, China Agricultural University	2009-2012
	Beijing, China	
B.S.	Plant Pathology, China Agricultural University	2005-2009
	Beijing, China	

Professional positions held

Teaching Assistant, University of Kentucky   Jan 2020-May 2020

Graduate Research Assistant, University of Kentucky   2014-2019

Teaching Assistant, New Oriental Education & Technology Group Inc., Beijing, China

2012-2013

Graduate Research Assistant, China Agricultural University, Beijing, China

2009-2012

Scholastic and professional honors

Recipient of Travel awards from American Society of Plant Biologists   2019

Recipient of Graduate School Fellowship from University of Kentucky   2014, 2015

Recipient of University Scholarships for Outstanding Students   2006, 2007, 2008

Recipient of Kingenta Special Scholarship   2007

Professional publications

Lim GH, Liu H, Yu K, **Liu R,** Baby S, Burch-Smith T, Mobley J, McLetchie N, Kachroo A, Kachroo P. (2020), The plant cuticle regulates apoplastic transport of salicylic acid during systemic acquired resistance. *Sci. Adv.* 6(19): eaaz0478.

Li D, **Liu R**, Singh D, Yuan X, Kachroo P, Raina R. (2019), JMJ14 encoded H3K4 demethylase modulates immune responses by regulating defense gene expression and pipecolic acid levels. *New Phytol.* doi:10.1111/nhp.16270.

Wang C, **Liu R**, Lim GH, de Lorenzo L, Yu K, Zhang K, Hunt AG, Kachroo A, Kachroo P. (2018), Pipecolic acid confers systemic immunity by regulating free radicals. *Sci. Adv.* 4(5): eaar4509. This work has been highlighted in Morning Ag Clips.

Li Y, **Liu R**, Zhou T, Fan Z. (2013), Genetic diversity and population structure of Sugarcane mosaic virus. *Virus Res.* 171: 242-246.